Received: 9 March 2023 | Revised: 18 July 2024 | Accepted: 12 August 2024

DOI: 10.1002/hbm.70010

RESEARCH ARTICLE

WILEY

Developmental patterns of inhibition and fronto-basal-ganglia white matter organisation in healthy children and children with attention-deficit/hyperactivity disorder

Mervyn Singh[1,2] | Patrick Skippen[3,4] | Jason He[1,2,5] | Phoebe Thomson[6,7,8] | Ian Fuelscher[1,2] | Karen Caeyenberghs[1,2] | Vicki Anderson[9] | Christian Hyde[1,2] | Timothy J. Silk[1,2,6]

[1]Cognitive Neuroscience Unit, School of Psychology, Deakin University, Geelong, Victoria, Australia

[2]Centre for Social and Early Emotional Development, Deakin University, Geelong, Victoria, Australia

[3]Neuroscience Research Australia, Randwick, New South Wales, Australia

[4]Hunter Medical Institute, Newcastle, New South Wales, Australia

[5]Department of Forensic and Neurodevelopmental Sciences, Sackler Institute for Translational Neurodevelopment, Institute of Psychiatry, Psychology, and Neuroscience, King's College London, London, UK

[6]Developmental Imaging, Murdoch Children's Research Institute, Melbourne, Victoria, Australia

[7]Department of Paediatrics, University of Melbourne, Melbourne, Victoria, Australia

[8]Autism Research Centre, Child Mind Institute, New York, New York, USA

[9]Royal Children's Hospital, Melbourne, Victoria, Australia

Correspondence
Mervyn Singh, Cognitive Neuroscience Unit, School of Psychology, Deakin University, 221 Burwood Highway, Burwood VIC 3125, Australia.
Email: mervyn.singh@deakin.edu.au

Funding information
National Health and Medical Research Council, Grant/Award Number: 1065895

Abstract

There is robust evidence implicating inhibitory deficits as a fundamental behavioural phenotype in children with attention-deficit/hyperactivity disorder (ADHD). However, prior studies have not directly investigated the role in which white matter properties within the fronto-basal-ganglia circuit may play in the development of inhibitory control deficits in this group. Combining recent advancements in brain-behavioural modelling, we mapped the development of stop-signal task (SST) performance and fronto-basal-ganglia maturation in a longitudinal sample of children aged 9–14 with and without ADHD. In a large sample of 135 ADHD and 138 non-ADHD children, we found that the ADHD group had poorer inhibitory control (i.e., longer stop-signal reaction times) across age compared to non-ADHD controls. When applying the novel parametric race model, this group effect was driven by higher within-subject variability (sigma) and higher number of extreme responses (tau) on stop trials. The ADHD group also displayed higher within-subject variability on correct responses to go stimuli. Moreover, we observed the ADHD group committing more task-based failures such as responding on stop trials (trigger failures) and omissions on go trials (go failures) compared to non-ADHD controls, suggesting the contribution of attentional lapses to poorer response inhibition performance. In contrast, longitudinal modelling of fixel-based analysis measures revealed no significant group differences in the maturation of fronto-basal-ganglia fibre cross-section in a subsample (74 ADHD and 73 non-ADHD children). Finally, brain-behavioural models revealed that age-related changes in fronto-basal-ganglia morphology (fibre cross-section) were significantly associated with reductions in the variability of the correct go-trial responses (sigma.true) and skew of the stop-trial distribution (tauS). However, this effect did not differ between ADHD and typically developing children. Overall, our findings support the growing consensus suggesting that attentional deficits subserve ADHD-related inhibitory dysfunction. Furthermore, we show novel evidence

suggesting that while children with ADHD are consistently performing worse on the SST than their non-affected peers, they appear to have comparable rates of neurocognitive maturation across this period.

KEYWORDS
ADHD, behavioural inhibition, developmental, dMRI, fixel-based analysis

Practitioner Points

1. Children with ADHD had poorer response inhibition (i.e., longer stop-signal reaction times), which was driven by higher within-subject variability than non-ADHD controls. ADHD children also displayed more variable responses to correct go trials than controls.
2. Children with ADHD committed more trigger-and-go failures on the SST, suggesting deficits in attentional processes.
3. Age-related changes in fronto-basal-ganglia fibre cross-section were associated with reductions in the variability and skewness of the stop-trial and correct go-trial responses across both ADHD and non-ADHD children.

1 | INTRODUCTION

Attention-deficit/hyperactivity disorder (ADHD) is a pervasive neurodevelopmental disorder characterised by higher levels of impulsivity, inattention, and hyperactivity (American Psychiatric Association, 2013; Faraone et al., 2015). ADHD has a current worldwide prevalence rate of ~5.9% in childhood (aged 18 and under) (Willcutt, 2012). ADHD often presents with deficits across multiple cognitive domains (Bloemsma et al., 2013; Claesdotter et al., 2018; Kofler et al., 2013, 2018, 2019; Lambek et al., 2011). Specifically, a seminal review proposed by Barkley (1997) posits that the behavioural presentation of ADHD may be driven by a fundamental deficit in the ability to constrain unwanted or inappropriate behaviours, commonly termed 'response inhibition'. This 'inhibition deficit model' of ADHD has been well supported across a range of studies and has since become one of the most popular accounts of explaining ADHD-related cognitive dysfunction (Bhaijiwala et al., 2014; Claesdotter et al., 2018; Slaats-Willemse et al., 2003). While it is true that there are well-replicated deficits in inhibitory control, a robust body of evidence has also linked ADHD to dysfunctions across a range of other cognitive domains, including working memory, planning and updating (Ramos et al., 2020), thus challenging the prevailing view that inhibitory control is a core deficit in the disorder.

Response inhibition in ADHD is commonly assessed using the stop-signal task (SST), a simple paradigm where individuals first develop a prepotent motor response which they must inhibit on a subset of trials (i.e., stop trials) when prompted by a salient stop signal (Matzke et al., 2018; Verbruggen, 2019; Verbruggen & Logan, 2008). Inhibitory performance on the SST is often formalised as a race between two competing processes, a go process that is triggered by the go stimuli, and a stop process that is triggered by the stop-signal (Logan & Cowan, 1984). Successful inhibition is thus dependent on the relative completion times of both processes. If the stop process finishes the race before the go process, then the response is inhibited. If the go process finishes first, then the response is maintained (Verbruggen & Logan, 2009). The underlying mathematical assumptions of the race model enable the covert latency of the stop trial distribution to be quantified as a stop-signal reaction time (SSRT), indexing the amount of time for an individual to successfully cancel their response after the stop signal is presented (Logan & Cowan, 1984; Verbruggen & Logan, 2009). Longer SSRTs are typically considered reflective of deficient inhibitory control and have been used as a sensitive behavioural marker for identifying response inhibition deficits in ADHD-diagnosed populations. Indeed, several meta-analyses have displayed robust evidence of prolonged SSRT in individuals with ADHD compared to typically developing individuals (Alderson et al., 2008; Kofler et al., 2013; Lijffijt et al., 2005; Lipszyc & Schachar, 2010; Oosterlaan et al., 1998), supporting Barkley's inhibitory deficit model of ADHD.

Traditional approaches to estimating SSRTs often rely on non-parametric techniques (i.e., mean estimation and integration methods), which summarise the stop-signal distribution using single measures (i.e., mean SSRT; Matzke et al., 2018; Verbruggen, 2019). Whilst easy to derive from the race model, summary measures are insensitive to interindividual fluctuations in performance at the trial-level, thereby masking crucial features of the data (Matzke et al., 2013). Alternative models of response inhibition have been developed to provide a more mechanistic account of inter-individual variability in SST performance. One such example is the parametric race model (Jana & Aron, 2022; Matzke, Love, & Heathcote, 2017; Matzke et al., 2013), a bespoke Bayesian estimation approach in which the entire distribution of go and stop trial RTs are fitted to an ex-Gaussian distribution, a commonly used distributional shape for RT data (Dawson, 1988). The ex-Gaussian distribution is a convolution of a normal Gaussian curve with an exponential tail, allowing for greater specificity in the characterisation of task performance through parameters that reflect the mean (mu), variability (sigma) and degree of skewness (tau) of the distribution (Matzke et al., 2013).

Additionally, successful response inhibition is not only contingent on how fast or consistent a behavioural response is stopped, but also on the reliability of 'triggering' the stop process (Band et al., 2003; Logan & Cowan, 1984; Hannah et al., 2023). For example, individuals who are unable to selectively attend to the stop-signal will perform worse on the SST than those who are able to successfully attend to the signal. These failures to successfully encode and discriminate the stop-signal, commonly known as trigger failures, are often considered to be reflective of a dysregulation in attentional processing (Jana & Aron, 2022 ; Matzke, Love, & Heathcote, 2017). Trigger failures have long been considered a contaminant of SSRT estimates and cannot easily be considered with non-parametric approaches (Matzke, Love, & Heathcote, 2017). Recent simulation work has evidenced that the presence of trigger failures can overestimate SSRT values by up to 100 ms (Band et al., 2003; Logan, 1994). Taken together, given that the bulk of the ADHD literature has used non-parametric SSRT measures, it is possible that prior findings of prolonged SSRT in this population may instead reflect deficits in attention-based processes rather than impaired motor-related stopping. More recent variants of the parametric race model allow for the simultaneous estimation of trigger failures during task performance, thus providing an avenue through which to disentangle the role of attentional-based contaminants on overall SST performance (Matzke, Love, & Heathcote, 2017; Matzke et al., 2019).

The advantages offered by the parametric race model have seen this approach used in a growing number of studies to provide novel interpretations of SST performance in healthy and clinical cohorts (Jana & Aron, 2022; Matzke, Hughes, et al., 2017; Mayes et al., 2021; Singh et al., 2022; Skippen, 2019). For example, in a recent longitudinal study of 138 typically developing children aged 9–14, we observed that developmental improvements in SSRT were driven primarily by reductions in sigma and tau of the stop trial distribution, implicating the role of reduced performance variability and the propensity of extremely slow responses towards overall inhibitory control efficiency (Singh et al., 2022). To date, only one study has directly applied the parametric race model to investigate the contribution of trigger failures in children with ADHD. Weigard et al. (2019) applied the parametric race model in a sample of 209 ADHD children aged 10 years. In addition to reporting greater variability and skew in both go and stop trial distributions (indexed by greater sigma and tau), the ADHD group also displayed a higher probability of engaging in trigger failures compared to non-ADHD controls. Relatedly, the ADHD group also displayed higher omissions on go trials, known as 'go failures', another performance characteristic commonly attributed to failures of attention during the SST. Furthermore, the authors showed that any group differences in SSRT were ameliorated after holding trigger failure constant, demonstrating that poor SST performance was predominantly due to poor sustained attention rather than a motor cessation (i.e., inhibitory) deficit, as might previously be assumed. These findings have considerable implications for the characterisation of inhibitory deficits in children with ADHD. However, as this study used a cross-sectional design, it is not able to determine whether findings reflect a persistent developmental trait in ADHD or a transient age-specific effect.

When speaking to the neurobiological mechanisms underpinning efficient stopping performance, a right lateralised network known commonly as the fronto-basal-ganglia circuit has been implicated in response inhibition (Aron, Durston, et al., 2007; Hannah & Aron, 2021). The fronto-basal-ganglia circuit is a triad of structurally connected regions comprising the right inferior frontal gyrus (rIFG), presupplementary motor area (preSMA) and subthalamic nucleus (STN) (Aron, Behrens, et al., 2007). Studies employing Diffusion Tensor Imaging (DTI) has evidenced significant correlations between indices of increased white matter (WM) organisation (i.e., fractional anisotropy; FA/radial diffusivity; RD) and reduced SSRT in WM underlying the right IFG, preSMA and STN (Aron, Behrens, et al., 2007; Aron, Durston, et al., 2007; King et al., 2012; Madsen, 2010; Madsen et al., 2020; Rae et al., 2015). More recently, previous work from our group has employed more advanced modelling techniques (namely, constrained spherical deconvolution [CSD] and fixel-based analysis [FBA]) in light of the well-documented 'crossing fibre problem' inherent in DTI (see Dhollander et al., 2021 for a detailed discussion). Using the novel FBA technique in a cross-sectional sample of healthy children aged 9, we identified a significant moderate association between reduced SSRT and increased fibre density (FD), a microstructural metric that quantifies intra-voxel axonal density (Dhollander et al., 2021), within the bilateral preSMA-STN and IFG-STN pathways of the circuit (Singh et al., 2021). In comparison, our follow-up longitudinal study found that despite an age-related increase in fibre-cross-section (FC), a morphological measure of fibre bundle size (Dhollander et al., 2021) in the bilateral preSMA-STN and IFG-STN pathways, fronto-basal-ganglia WM maturation was not associated with improvements in SST performance (Singh et al., 2022).

Large-scale disruptions in structural–functional networks within the brain are thought to underlie the behavioural presentation of ADHD (Ball et al., 2019; Cai et al., 2018). Given this, there has been an increased focus on understanding the role of WM networks in ADHD symptomatology. However, studies of such differences have yielded inconsistent results, with some evidencing lower FA or fixel metrics (FD/FC) in several tracts implicated in higher-order sensorimotor processing, cognitive control and attentional networks (Aoki et al., 2018; Chen et al., 2016; Fuelscher et al., 2021; Hyde et al., 2021), while others show the opposite direction (Li et al., 2010; Peterson et al., 2011) or no significant effects (Sudre et al., 2023). Despite response inhibition deficits being a fundamental behavioural phenotype in ADHD, no study has directly investigated whether disruptions within the fronto-basal-ganglia circuit might explain poor SST performance commonly seen in this population. Indirect work employing DTI-based approaches has shown no significant group differences between ADHD and typically developing children with respect to WM and SSRT at the whole brain, or tract of interest level (corpus callosum, sagittal striatum, superior longitudinal fasciculus; Albajara Senz et al., 2020; Bessette & Stevens, 2019; Tremblay et al., 2020). Furthermore, the vast majority of previous work has employed

cross-sectional samples, which are limited to only static links between brain-behavioural outcomes (Mills & Tamnes, 2014). Given that both executive functioning and WM structural properties undergo rapid development during childhood (Goddings et al., 2021), employing a longitudinal approach will allow for a more comprehensive approach to capturing potential differences in the developmental trajectories of inhibition and white matter properties in ADHD relative to controls.

The lack of consistent findings may likely reflect variations in sample size, clinical presentation (e.g., subtype), and methods of analysis. Therefore, a unified account of WM organisation in ADHD as well as its behavioural consequences, continue to be elusive. Further, despite evidence supporting the functional role of the fronto-basal-ganglia circuit in facilitating response inhibition, the exact neural mechanisms of this network are still being debated in the literature. Whilst the rIFG's role in action-stopping is to purportedly recruit the STN via the hyper-direct pathway from rIFG to basal ganglia (Chen et al., 2020; Jahfari et al., 2011; Rae et al., 2015), a series of functional imaging studies have also reported comparable neural activity in the rIFG on tasks that have no overt inhibitory demands (Hampshire et al., 2010; Hampshire, 2015). More recently, an electroencephalography (EEG) study by Choo et al. (2022) found evidence that rIFG lesions were associated with an increase in trigger failures, suggesting that its role appears to be more attentional based (i.e., in the triggering or initiation of a cascade leading to motor cessation).

To this end, the present work sought to clarify prior findings by modelling longitudinal group differences in response inhibition and WM organisation in children with and without ADHD. Our aims were threefold: First, we attempted to examine the developmental progression of inhibitory control in both ADHD and non-ADHD children. As per previous work (Alderson et al., 2007; Lipszyc & Schachar, 2010), we expect inhibitory deficits to be consistent in the ADHD group over time compared to non-ADHD controls, as reflected in prolonged SSRT. Given the methodological limitations of non-parametric SSRT, we then applied the parametric race model to disentangle the role of attentional-based components from overall inhibitory control. By using the parametric race model (Matzke et al., 2013, 2019), we hypothesised that prolonged SSRTs in children with ADHD would be driven by greater within-subject variability (sigma) and more extreme responses (tau) relative to non-ADHD controls. In line with recent evidence suggesting that attentional deficits may underlie poor response inhibition in ADHD (Weigard et al., 2019), we also expected that children with ADHD would commit more trigger-and-go failures over age. Second, we leveraged the novel FBA framework to explore the developmental progression of fibre-specific properties underlying the fronto-basal-ganglia circuit across ADHD and non-ADHD children. We propose that children with ADHD would show altered maturational processes within the fronto-basal-ganglia circuit (indexed as lower FD and FC across age) compared to controls. Finally, we explored whether different maturational profiles of fronto-basal-ganglia WM in ADHD may subserve response inhibition deficits in this group. Here, we hypothesized that lower FD and FC in children with ADHD will be predictive of poorer SST performance in this group.

2 | MATERIALS AND METHODS

2.1 | Participants

The current study used a subset of data obtained from the Children's Attention Project (CAP) (Sciberras et al., 2013), and its neuroimaging arm, the Neuroimaging of the Children's Attention Project (NICAP) (Silk et al., 2016). Participants recruited into NICAP were sourced from the 36-month follow-up of the larger CAP study. The NICAP sample underwent concurrent cognitive testing and MRI imaging over three sessions every 1.5 years at the Murdoch Children's Research Institute. Written consent was given by the parent/guardian prior to data collection. During data collection, participants were excluded if they presented with any of the following: intellectual disability; serious medical conditions; genetic disorders; moderate–severe sensory impairment; neurological problems; and parents with insufficient English to complete interviews/questionnaires (Silk et al., 2016). ADHD diagnosis was confirmed using the parent/guardian report NIMH Diagnostic Interview Schedule for Children-IV (DISC-IV) (Shaffer et al., 2000) at baseline of the CAP study, and the first and third sessions of the NICAP study (timepoint 1 and 3). Children presenting with a history of ADHD (i.e., positive ADHD diagnosis at CAP baseline and/or NICAP timepoint 1) were considered part of the ADHD group. Children who did not meet ADHD diagnostic criteria at both timepoints were considered as non-ADHD controls. The presence of internalizing (e.g., depression) or externalizing problems (e.g., oppositional defiant disorder) was assessed using the DISC-IV during diagnostic assessment (Shaffer et al., 2000). Finally, children were not asked to cease medication for during data collection so as to provide a naturalistic environment (i.e., 'classroom' setting) in which cognitive performance can be assessed. Medication history and dosage information were recorded during the assessment by research staff blinded to each participant's diagnosis. Detailed information on the types of medication taken by ADHD and non-ADHD participants at each timepoint are presented in Tables S4 and S5 of Supporting Information A.

For the purposes of our study, participants without SST data for at least one timepoint were excluded from the analysis. Based on these criteria, we obtained a sample of 153 ADHD and 177 non-ADHD children with SST data for at least one timepoint. Following quality control procedures (see below sections), the final sample consisted of 135 ADHD and 138 non-ADHD participants (Figure S1a; Supporting Information A). Of this final sample, a sub-group of 88 ADHD and 80 non-ADHD participants also had diffusion MRI data for at least one timepoint. After quality assessment procedures (see below sections), the final neuroimaging sub-sample consisted of 74 ADHD and 73 non-ADHD participants who had MRI data for up to three timepoints (Figure S1b; Supporting Information A).

2.2 | Stop-signal task

The SST was administered using the open-source STOP-IT version of the task (Verbruggen et al., 2008). STOP-IT consists of 192 trials, of which 144 (75%) are go trials and 48 (25%) are stop trials. Go trials consist of a single fixation cross displayed at the centre of the screen for 250 ms followed by a series of shapes (square or circle) presented at the same location for 1250 ms. Participants were instructed to respond to these as quickly and accurately as possible, pressing the 'Z' key on a standard computer keyboard with their left index finger when presented with a square, or the '?' key with their right index finger when presented with a circle. On stop trials, the go stimulus was followed by an auditory stop-signal (750 Hz) presented at variable delays. Upon hearing the stop-signal, participants must cease any response and wait for the following go-trial to resume. The duration of stop-signal delays (SSDs) varied systematically across stop trials via a staircasing algorithm. Following an initial duration of 250 ms for all participants, SSDs increased or decreased by increments of 50 ms according to a participant's performance on the preceding stop trial, converging on a ~50% probability of inhibiting on a given stop-signal. STOP-IT is freely available for download at the following link: https://github.com/fredvbrug/STOP-IT.git.

2.3 | MRI acquisition

Diffusion MRI data were acquired at each of the three timepoints using a 3T Siemens scanner with a 32-channel head coil. The following parameters were used for the diffusion MRI sequence at all three timepoints: plane = transverse; phase-encoding direction = anterior–posterior; multiband factor = 3; *b* value: $b = 2800$ s/mm^2; gradient directions = 60 (with 4 interleaved *b*0 volumes); voxel size = 2.4 mm^3 isotropic; echo-time/repetition time (*TE*/*TR*) = 110/3200 ms; acquisition matrix = 110 × 100; bandwidth = 1758 Hz. Two *b*0 reverse-phase encoded blip images were acquired to correct for susceptibility distortions (Andersson & Sotiropoulos, 2016). In addition to diffusion data, T1-weighted anatomical MRI data was also collected in the sagittal plane using the following protocol: Magnetization-Prepared Rapid Acquisition Gradient Echo (MPRAGE), *TR* = 2530 ms; *TE* = 1.77, 3.51, 5.32, 7.2 ms; flip angle = 7°; voxel size = 0.9 mm^3; field of view = 230 mm^2 with in-scanner motion correction. Data for timepoints 1 and 2 were acquired on a TIM Trio scanner whilst data for timepoint 3 was acquired following an upgrade to the MAGNETOM Prisma scanner. All scanning parameters remained consistent pre- and post-scanner upgrade, however, to adjust for potential effect of scanner type on our statistical analyses, scanner upgrade was included as a covariate in our longitudinal models.

2.4 | Covariates

Prior studies have shown response inhibition to be differentially associated with sex (Mansouri et al., 2016; Ribeiro et al., 2021), socioeconomic status (SES; Last et al., 2018; Lawson et al., 2018) and use of stimulants (e.g., methylphenidate; Bedard et al., 2003; Brackenridge et al., 2011; Coghill, 2010). As such, these were included in our longitudinal models as covariates of no interest. Sex was collected as a self-report measure at the start of each testing session. SES was recorded at each session using the Index of Relative Socio-economic Advantage and Disadvantage (IRSAD), a measure of relative socio-economic disadvantage in Australia with a mean of 1000 and a standard deviation of 100. Lower IRSAD scores indicate areas with a greater incidence of disadvantage (Australian Bureau of Statistics, 2013). Medication use information was recorded by the researchers at the end of each session. In addition, subject-specific variability in head size and movement in the MRI scanner can have significant impacts on the validity of diffusion MRI measures (Baum et al., 2018; Kijonka et al., 2020; Thomson et al., 2021). Hence, our imaging and brain-behavioural models were also adjusted for these variables. In-scanner head motion (indexed as mean framewise displacement; mean FWD) was calculated for each participant's raw diffusion MRI data (excluding b0 shells and the reference volume) following the approach by Power et al. (2012) in FSL (v. 6.0.1). We also calculated the mean estimated intracranial volume (eTIV) in each participant's pre-processed T1-weighted image using the recon-all function in FreeSurfer (v. 6.0; Fischl, 2012).

2.5 | SST data preparation

2.5.1 | SST quality control

To ensure that only participants who adequately completed the task entered the final model, SST data were quality assessed using stringent cut-off criteria following the same procedures as our previous work (Singh et al., 2022; See Figure S2 and Table S2 of Supporting Information A for a list of participants that were removed). Participants were removed if they: (1) did not complete the task (<192 trials); (2) proactively slowed their performance >300 ms on go trials over the course of the task; (3) displayed an overall probability of >75% in responding to stop signals. In addition, we (4) visually checked if the staircase tracking algorithm was performing adequately for each participant by plotting their probability of responding to stop signals against the range of SSDs they obtained across the task. Participants were retained if there was a systematic increase in probability of responding to stop signal with SSD. For appropriate estimation of incorrect responses on go trials (i.e., mu.false, sigma.false, tau.false), we also excluded participants who displayed (5) no-choice errors on go trials. Finally, following the estimation of SST parameters (see below), we removed an additional two observations (timepoint 1 = 1; timepoint 3 = 1) from the non-ADHD group due to missing age data, and three observations (timepoint 1 = 1; timepoint 2 = 1; timepoint 3 = 1) from the ADHD group for missing SES data.

2.5.2 | Parametric modelling of SST performance

SST performance was modelled using a variant of the parametric race model known as the ex-Gaussian 3 (EXG3; Matzke et al., 2019). The

EXG3 estimates mu, sigma, and tau parameters for the stop process, as well as for correct (i.e., 'true') and incorrect (i.e., 'false') responses separately for go trials. Further, the model also simultaneously accounts for the probability (%) of trigger failures (indexing responses to stop trials) and go failures (indexing omissions on go trials) as separate, quantifiable parameters. We used an individual modelling approach, whereby go, stop and attention-related parameters (trigger and go failures) were estimated separately for each participant at each timepoint. This was done to maintain the independence of observations in our data during subsequent statistical modelling via GAMMs (see Section 2.8.1). This resulted in a total of 11 parameters for each participant (Table S1; Supporting Information A). We also computed traditional SST metrics by using the parameters obtained from the EXG3 model. Specifically, we calculated SSRT and go reaction time (GoRT) by adding mu and tau of the stop trial and correct go trial distributions, respectively. All estimation procedures were conducted in R using the Dynamic Models of Choice package (DMC; Heathcote et al., 2019). The DMC package employs a Bayesian parametric estimation approach for modelling participant-level EXG3 parameters. A detailed discussion of the rationale underlying Bayesian parametric estimation is beyond the scope of this article; the reader is directed to the following sources for further information (Annis & Palmeri, 2018; van de Schoot et al., 2014). The end goal of Bayesian modelling is the posterior distribution, a probability distribution that reflects the contribution of both prior knowledge and the observed evidence (data) for a parameter of interest (van de Schoot et al., 2014).

Following the steps of Matzke et al. (2019), we assumed weakly informative priors for the subject-level parameters, which closely match those of Heathcote et al. (2019). These prior distributions were then updated by the observed data to yield posterior distributions through a sampling technique known as Differential-Evolution Markov Chain Monte-Carlo (DE-MCMC; Turner et al., 2013). We ran the sampling scheme across three stages. First, we ran an initial burn-in period of 500 iterations for each of the 33 chains (by default, DMC samples three times as many chains as there are parameters) with 5% migration to correct for instances where chains were 'stuck' during the sampling process, increasing the probability of parameters being sampled in the appropriate space, thus improving the likelihood of convergence. However, samples derived from migration can often bias estimates to higher-likelihood regions, and thus, cannot be used. Therefore, we ran a second burn-in of an additional 500 iterations with migration off. Finally, a final sample of 400 iterations was run until chains were converged, which were then retained for further analysis. Convergence of chains was assessed visually via trace plots and statistically using Gelman–Rubin R^ values (Gelman & Rubin, 1992). Chains were adequately converged if the trace-plots did not contain systematic deviations across the parameter space (i.e., if all chains were spread equally across the sampling scheme), and if the R^ values were <1.1. Summary statistics (medians) from each subject's posterior distribution for each parameter were extracted from the final set of 400 chains. These were then used as dependent variables in our longitudinal statistical models. Figures S3–S8 of Supporting Information A visualizes the subject-level posterior distributions for the (1) matching go process (i.e., GoRT; mu.true + tau.true), (2) mismatching go process (mu.false + tau.false), (3) stop-process (i.e., SSRT; muS + tauS), (4) go failures and (5) trigger failures.

2.5.3 | Final behavioural sample

After quality control procedures, the final behavioural sample consisted of 135 ADHD and 138 non-ADHD participants. A flow diagram of the quality control procedure for the behavioural sample is presented in Figure S2 of Supporting Information A. Sample characteristics for the behavioural cohort are presented in Table 1.

2.6 | Diffusion MRI data preparation

2.6.1 | Pre-processing and quality assessment

Analysis of the diffusion MRI data was conducted on a subset of 88 ADHD and 80 non-ADHD participants. All diffusion MRI processing and analysis were conducted in MRtrix3tissue (https://3tissue.github.io/), a fork of the MRtrix3 project (Tournier et al., 2019) using the Monash High Performance Computing Cluster (Goscinski et al., 2014). Diffusion data were pre-processed using an in-house automated script developed by the research team and closely followed the recommended pipeline for FBA (Dhollander et al., 2021). This script is available for public use (see 'Code and Data availability'). Specifically, the pre-processing pipeline involved the following steps: denoising (Veraart et al., 2016), Gibbs Unringing (Kellner et al., 2016) and correction of geometric distortions with slice-to-volume motion correction and outlier replacement (Andersson et al., 2003, 2016, 2017; Andersson & Sotiropoulos, 2016). The pre-processed data were then quality assessed by a team of researchers (N.V., I.F., L.D., S.S., P.T., M.S.) for the presence of subject motion (as indexed by substantial Venetian blinds artefacts), masking issues, and otherwise corrupted volumes within the data. A total of 15 ADHD and 12 non-ADHD observations were subsequently removed from further analysis (see Figure S9 and Table S3 of Supporting Information A for more details). Following the implementation of the FBA pipeline, we also removed participants who were missing T1-weighted data, as we could not calculate eTIV values for these participants.

2.6.2 | Single-shell 3-tissue CSD and population template

Group-averaged response functions for each tissue-type (WM, grey matter [GM], and cerebrospinal fluid [CSF]) were extracted for each subject and Single-shell 3-Tissue Constrained Spherical Deconvolution (SS3TCSD) was conducted to obtain WM-like Fibre Orientation Directions (FODs; Dhollander et al., 2016). Further, group-level global

TABLE 1 Sample characteristics of the behavioural cohort.

Measure	Non-ADHD control	ADHD	Difference *p*-value
N (*n* datapoints)	138 (209)	135 (238)	–
Participants, count (% male)			
T1	115 (58.3%)	112 (66.1%)	–
T2	60 (55%)	69 (79.7%)	–
T3	34 (61.8%)	57 (70.2%)	–
Age, mean (SD)			
T1	10.47 (0.51)	10.44 (0.53)	.58
T2	11.81 (0.52)	11.72 (0.54)	.35
T3	13.07 (0.49)	13.24 (0.67)	.23
Conners ADHD Index, mean (SD)			
T1	1.80 (3.56)	10.49 (6.49)	**<.001**
T2	1.32 (1.91)	10.31 (6.42)	**<.001**
T3	0.47 (1.16)	8.33 (6.87)	**<.001**
Baseline internalization, count, yes (% yes)			
T1	6 (5.2%)	24 (21.8%)	–
T2	6 (10%)	16 (23.5%)	–
T3	4 (11.8%)	12 (21.1%)	–
Baseline externalization, count, yes (% yes)			
T1	15 (13%)	46 (41.8%)	–
T2	8 (13.3%)	36 (52.9%)	–
T3	1 (2.9%)	28 (49.1%)	–
SES, mean (SD)			
T1	1021.33 (42.95)	1012.90 (47.22)	.26
T2	1024.73 (45.97)	1018.23 (41.13)	.36
T3	1015.82 (40.42)	1018.28 (40.71)	.85
Medication status, count, yes (% yes)			
T1	2 (1.9%)	25 (25%)	–
T2	1 (1.7%)	23 (33.8%)	–
T3	0 (0%)	11 (24.4%)	–

Note: Conners ADHD Index Score obtained from the Conners 3rd Edition Parent Report scale (Conners et al., 2011). Difference *p* values reported from Mann–Whitney *U* tests. Bold indicates significant group differences.
Abbreviations: SD, standard deviation; SES, socioeconomic status.

intensity normalisation and bias-field correction were conducted to improve inter-subject comparability of FOD amplitudes. We subsequently generated a study-specific population template from the cohort that passed quality control checks (80 ADHD and 75 non-ADHD participants). The population template was then transformed to standard space (Montreal Neurological Institute [MNI]) using the FSL FA template following a similar approach to our previous longitudinal study in typically developing children (Singh et al., 2022).

2.6.3 | Tract-of-interest fixel-based analysis

To delineate our fronto-basal-ganglia circuit, we adopted the same procedures as described in our previous work (Singh et al., 2021, 2022). Briefly, our cortical ROIs (IFG and preSMA) were parcellated in each hemisphere using the Ranta Frontal Lobe atlas (Ranta et al., 2014), while the STN was delineated using the STN atlas (Keuken & Forstmann, 2015). We applied probabilistic tractography to estimate streamlines connecting the IFG-preSMA, IFG-STN and preSMA-STN in each hemisphere using the following parameters (angle = 22.5°, max length = 250 mm, min length = 10 mm, power = 1.0, FOD cut-off = 0.1, streamline selection = 2000). We also applied exclusion ROIs in the coronal slice of the left hemisphere and posterior region of the brain to mitigate spurious streamlines. A visual representation of the bilateral IFG-preSMA, preSMA-STN and IFG-STN tracts is presented in Figure 1. In preparation for subsequent statistical analysis, each tract was segmented into individual fixel masks. Finally, we calculated mean FD and FC values across all fixels in each tract per participant. As per the recommended steps for FBA (Dhollander et al., 2021; Raffelt et al., 2017), FC values were further

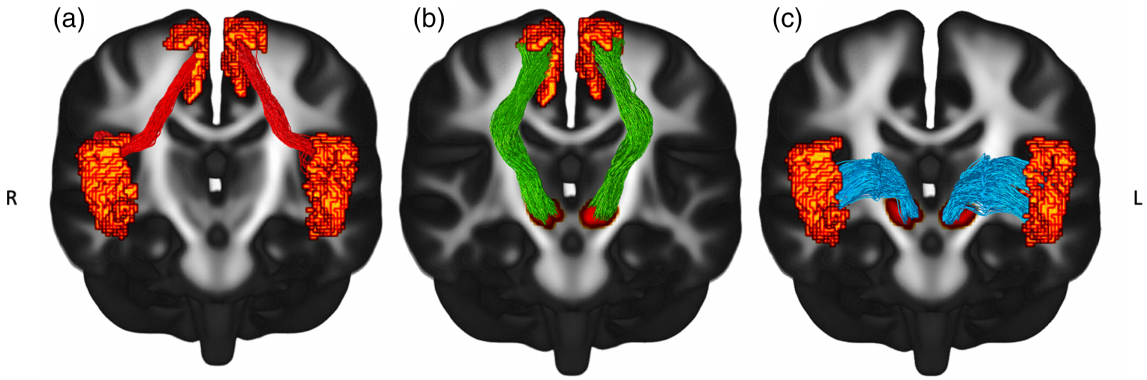

FIGURE 1 Visual representation of the bilateral fronto-basal-ganglia circuit overlaid on the population template. IFG, Inferior frontal gyrus; pre-SMA, Presupplementary motor area; STN, subthalamic nucleus.

log-transformed (FC (log)) to ensure normality of data across participants (Dhollander et al., 2021).

2.6.4 | Final neuroimaging sample

After quality assessment and other removal procedures, a final sample of 74 ADHD and 73 non-ADHD participants were entered into the models. A flow diagram of the quality control procedure for the neuroimaging sample is presented in Figure S9 with further exclusion details listed in Table S3 of Supporting Information A. Sample characteristics for the imaging cohort are presented in Table 2.

2.7 | Attrition analyses

Attrition analyses of SST performance were conducted to examine if better-performing participants were retained across the three data collection timepoints. Results revealed that there were no significant differences between non-ADHD children attending one, two or three timepoints in baseline SST performance in both the behavioural and imaging samples (Tables S6 and S7; Supporting Information A). ADHD children in the behavioural cohort who had completed all three timepoints had significantly higher mean of the correct go trial response (mu.true) compared to children with only one timepoint ($M(diff) = 75.47$; $p(adj) = .03$). Further, ADHD children in the behavioural sample with three timepoints had significantly lower skew of the correct go trial response (tau.true) than children with one timepoint ($M(diff) = -43.01$; $p(adj) = .001$). ADHD children in the imaging subsample with two timepoints also displayed lower exponential skew of the correct go-trial responses (tau.true) than those with one timepoint ($M(diff) = -53.13$; $p(adj) = .02$). ADHD children in the imaging sample with all three timepoints had lower exponential skew of the correct go trial responses (tau.true) than those with two timepoints ($M(diff) = -54.16$; $p(adj) = .03$; Tables S8 and S9; Supporting Information A).

2.8 | Analytical procedure

2.8.1 | Developmental trajectories of inhibitory control

Developmental patterns of response inhibition in children with and without ADHD were assessed using generalised additive mixed models (GAMMs; Hastie & Tibshirani, 1990), a data-driven statistical framework that flexibly models non-linear relationships (Wood, 2011, 2017). All analyses were conducted with maximum likelihood (ML) estimation within the 'mgcv' package in R (Wood, 2017). EXG3-derived parameter estimates of the go and stop trial distributions were used as measures of interest, with the latter (i.e., stop trial parameters) specifically used as indices of response inhibition. Using a stepwise design, models assessing the main effect of (1) age, (2) group (i.e., ADHD, non-ADHD controls), and (3) the interaction of age and group were entered iteratively into the analysis following an initial 'null' model for each outcome variable. Separate models were also run using univariate SST performance measures (GoRT and SSRT) as outcomes of interest to compare between approaches. Like our previous work in a typically developing sample (Singh et al., 2022), age was modelled as a smooth term with a penalized cubic regression spline and basis dimension of 4 to capture potential non-linear trajectories with SST performance. We adjusted for sex, SES and medication use in our models. Prior to analysis, all categorical covariates were included as ordered factors to easily compare between contrasts (i.e., between ADHD and non-ADHD groups), while continuous variables were mean-centred to standardize all units of measurement in our models.

2.8.2 | Developmental trajectories of fronto-basal-ganglia WM

Longitudinal changes in FD and FC (log) of the fronto-basal-ganglia circuit were evaluated using a series of nested GAMM models. Starting from a 'null' model, more complex models were run to investigate

TABLE 2 Sample characteristics of the imaging cohort.

Measure	Non-AHD control	ADHD	Difference *p*-value
N (*n* datapoints)	73 (116)	74 (138)	–
Participants, *count* (*% male*)			
T1	38 (68.4%)	51 (66.7%)	–
T2	51 (54.9%)	54 (79.6%)	–
T3	27 (66.7%)	33 (72.7%)	–
Age, *mean* (*SD*)			
T1	10.38 (0.46)	10.41 (0.46)	.52
T2	11.78 (0.53)	11.72 (0.56)	.58
T3	13.04 (0.51)	13.32 (0.76)	.12
Conners ADHD Index, *mean* (*SD*)			
T1	1.82 (3.51)	9.73 (6.34)	**<.001**
T2	1.20 (1.72)	10.37 (6.66)	**<.001**
T3	0.30 (0.82)	8.06 (7.08)	**<.001**
Baseline internalization, *count*, *yes* (*% yes*)			
T1	3 (7.9%)	10 (20%)	–
T2	4 (7.8%)	10 (18.9%)	–
T3	3 (11.1%)	6 (18.2%)	–
Baseline externalization, *count*, *yes* (*% yes*)			
T1	5 (13.2%)	25 (50%)	–
T2	5 (9.8%)	26 (49.1%)	–
T3	1 (3.7%)	13 (39.4%)	–
SES, *mean* (*SD*)			
T1	1025.87 (45.15)	1018.00 (39.02)	.32
T2	1021.69 (48.16)	1020.06 (39.09)	.82
T3	1018.04 (41.67)	1018.79 (40.29)	.91
Medication status, *count*, *yes* (*% yes*)			
T1	1 (2.6%)	14 (27.5%)	–
T2	0 (0%)	18 (33.3%)	–
T3	0 (0%)	6 (18.2%)	–
Framewise displacement, *mean* (*SD*)			
T1	0.99 (0.25)	0.96 (0.18)	.66
T2	0.80 (0.12)	0.89 (0.20)	**<.05**
T3	1.03 (0.18)	0.99 (0.14)	.62
Estimated total intracranial volume, *mean* (*SD*)			
T1	1,634,084.5 (117,478.4)	1,591,464.6 (139,093.4)	.14
T2	1,592,624.9 (143,446.1)	1,597,655.4 (143,891.8)	.91
T3	1,593,501.3 (136,787.3)	1,606,285.2 (150,626.9)	.47

Note: Conners ADHD Index Score obtained from the Conners 3rd Edition Parent Report scale (Conners et al., 2011). Difference *p* values reported from Mann–Whitney *U* tests. Bold indicates significant group differences.

Abbreviations: SD, standard deviation; SES, socioeconomic status.

the relationship between (1) age, (2) group and the (3) interaction between age and group on WM maturation within the fronto-basal-ganglia circuit. These models were conducted separately for FD and FC (log) in each tract of interest: (1) IFG-preSMA, (2) preSMA-STN and (3) IFG-STN for both hemispheres. All neuroimaging models were conducted using maximum likelihood (ML) estimation. Age was modelled as a smooth term with a penalized cubic regression spline and basis dimension of 4 following the same procedures as above. We adjusted for sex, SES, and medication status across all models. Further, mean head motion (mean FWD), total brain volume (eTIV) and scanner upgrade were included as additional covariates of no-interest in our models.

2.8.3 | Predicting change in response inhibition from change in fronto-basal-ganglia WM

Brain-behaviour associations between changes in fronto-basal-ganglia WM and response inhibition were conducted using a similar approach as our study previous study in typically developing children (Singh et al., 2022). The yearly rate-of-change in FD/FC (log) for tracts identified as significant in our neuroimaging-only models were extracted as a random slope per participant. This was achieved by running a series of linear mixed-effect models predicting change in fronto-basal-ganglia WM from age (adjusting for mean FWD and eTIV). Steeper random slopes indicate a greater yearly rate-of-change in FD/FC (log). These slopes were then included as predictors in a series of nested GAMMs to examine whether the addition of WM development rate predicts composite measures of SST performance (SSRT; GoRT), and parameters derived from the parametric race model. Note that we selected outcome measures for SST performance only if they were significant in the behavioural-only GAMMs (as per Section 2.8.1). Following a stepwise approach similar to Sections 2.8.1 and 2.8.2, we ran a (1) 'null' model (initial best-fitting model for the behavioural-only GAMMs), a (2) main-effect model (addition of FD/FC (log) slope as a main effect), and an (3) age-by-FD/FC (log) interaction model. This latter model represents a linear interaction between the smooth age term and FD/FC (log) slope, informing us whether individual differences in fronto-basal-ganglia maturation are associated with different rates of SST performance over age. SES, sex, medication status and the effect of scanner type were included as nuisance covariates in all models.

2.8.4 | Model comparison

For all models run in the present work, a series of comparisons were undertaken to determine the most parsimonious model. The compareML function from the 'itsadug' R package was used to compare all models in our analysis (van Rij et al., 2015), following similar approaches by Vijayakumar et al. (2021). The compareML function evaluates model-fit based on a χ^2 test on the difference in scores and degrees of freedom. More complex models were selected if the result of the χ^2 test was significant at $p < .05$ when compared to a lower-order model. Due to the substantial number of comparisons conducted for the neuroimaging GAMMs, p values for all parametric and smooth coefficients, and model comparisons were adjusted using the false discovery rate (FDR) correction method ($p_{FDR} = .05$). Statistical details of all model comparisons conducted for the main analysis are presented in Tables S1–S30 of Supporting Information B.

2.8.5 | Sensitivity analyses

In addition to our main analysis, we also conducted several sensitivity analyses to assess the robustness of our results. First, given that comorbidity rates are often high in the ADHD population, we sought to examine whether the presence of internalizing or externalizing problems collected during diagnostic assessment was predictive of brain-behavioural relationships (T. Due to the unbalanced number of observations across timepoints, we elected to only include the presence of comorbidities at CAP baseline as covariates in our sensitivity analysis. This mirrored the approach of a recent publication by Thomson et al. (2022b) who had leveraged the same dataset in their manuscript. Results of this sensitivity analysis are presented in Tables S10-S15 of Supporting Information A. Second, as we have included children with a history of ADHD in our sample, it is possible that our findings may have been influenced by children who have remitted since their initial diagnosis. Indeed, some studies have demonstrated comparable task-related performance in ADHD-remitted participants to neurotypical controls (Michelini et al., 2016). For this second sensitivity analysis, we re-analyzed our main results after the removal of ADHD participants that have remitted by their last timepoint. For the behavioural sample, this resulted in a removal of 55 participants from a total of $n = 135$ ADHD children (leaving 80 with persistent ADHD [138 datapoints]). For the imaging subsample, we removed 30 participants from a total of $n = 74$ ADHD children (leaving 44 with persistent ADHD [81 datapoints]). Figure S10 of Supporting Information A visualizes the frequencies of ADHD participants who had either remitted at NICAP recruitment (timepoint 1; behavioural sample = 27; neuroimaging subsample = 6) or at the third diagnostic follow-up (timepoint 3; behavioural sample = 28; neuroimaging subsample = 24). Results are presented in Tables S16-S22 of Supporting Information A.

3 | RESULTS

3.1 | Developmental trajectories of inhibitory control

3.1.1 | Go trial performance

Longitudinal modelling of go trial performance indicated a significant age-effect for GoRT, whereby reaction times for go responses improved with age (Figure 2a; Table 3). However, inclusion of a main effect for group did not significantly improve the model, suggesting that both ADHD and non-ADHD children report similar go-trial performance. Likewise, evaluation of the EXG3 model parameters revealed significant age-effects for the Gaussian mean of the correct response (mu.true; Figure 2b; Table 3). The gaussian variability of the correct response (sigma.true) displayed a significant group effect, with higher variability in the ADHD group relative to controls (Figure 2c; Table 3). This latter effect was consistent across age. No models were significant for the exponential tail of the correct response (tau.true),

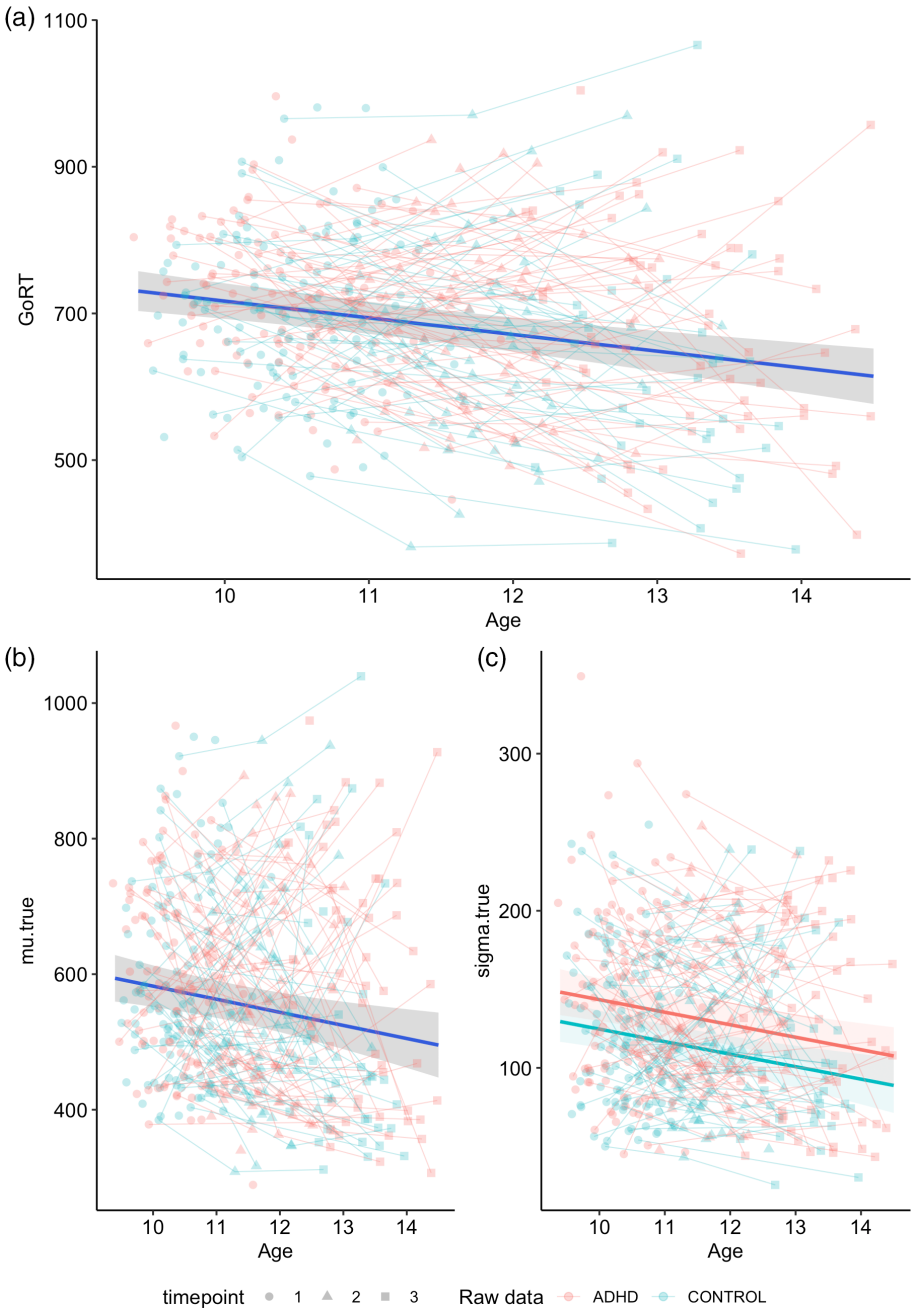

FIGURE 2 Best-fitting models of the go trial parameters. (a) Age main-effect model for GoRT; (b) age main-effect model for mu.true; (c) group main-effect model for sigma.true. Age in years; GoRT, mu.true, sigma.true in ms.

nor for any parameters of the incorrect go-trial distribution (see Tables S1–S7 of Supporting Information B).

3.1.2 | Stop trial performance

Model comparisons for Stop-trial performance metrics are presented in Tables S8–S11 of Supporting Information B. Results for the stop-trial metrics revealed that the ADHD group had significantly longer SSRT values than the non-ADHD group (Figure 3a; Table 4). This was paralleled by a significant main effect of group on the Gaussian means (muS), variability (sigmaS) and exponential tail (tauS) of the stopping distribution (Figure 3b–d; Table 4). For the best-fitting models across all metrics, both ADHD and non-ADHD groups also displayed significant consistent age-related improvements across the developmental span.

3.1.3 | Task-based failures

Model comparisons for task-based failure parameters are provided in Tables S12 and S13 of Supporting Information B. The inclusion of a main effect for group significantly improved model fit for both trigger (Prob_TF) and go failures (Prob_GF; Figure 4a,b; Table 5). The ADHD group had a higher probability of committing both trigger and go failures than non-ADHD controls. SES, medication status and sex did not significantly predict the probability of trigger or go failure for any best-fitting models.

TABLE 3 Parametric and smooth terms for the best-fitting models for go trial parameters.

	GoRT			mu.true			sigma.true		
Parametric coefficients	***Est. (SE)***	***t***	***p***	***Est. (SE)***	***t***	***p***	***Est. (SE)***	***t***	***p***
Intercept	684.69 (11.22)	61.05	**<.001**	555.08 (14.09)	39.39	**<.001**	132.15 (6.45)	20.50	**<.001**
Group	–	–	–	–	–	–	−18.73 (6.44)	−2.91	**<.001**
SES_c	−0.14 (0.16)	−0.90	.37	−0.03 (0.20)	−0.16	.87	−0.06 (0.07)	−0.80	.43
med	−1.70 (18.57)	−0.09	.93	−2.06 (23.36)	−0.09	.93	1.39 (8.83)	0.16	.88
Sex	6.29 (14.12)	0.45	.66	22.17 (17.73)	1.25	.21	8.17 (6.38)	1.28	.20
Smooth terms	***Edf (Ref.df)***	***F***	***p***	***Edf (Ref.df)***	***F***	***p***	***Edf (Ref.df)***	***F***	***p***
s(age_c)	1.00 (1.00)	23.55	**<.001**	1.00 (1.00)	10.40	**<.001**	1.01 (1.01)	15.01	**<.001**
s(SID)	111.83 (256.00)	0.89	**<.001**	104.88 (256.00)	0.78	**<.001**	122.39 (255.00)	1.02	**<.001**

Note: Est.: estimated regression parameter; SE: standard error; edf: estimated degrees of freedom; Ref.df: reference degrees of freedom; Group: ADHD and controls; SES_c: mean-centred SES; med: medication status; sex: males and females; s(age_c): smoothed mean-centred age; s(SID): subject ID entered as a random effect. GoRT: Go trial reaction time; Mu.true: mu of the correct go trial reaction time distribution; sigma.true: sigma of the correct go trial reaction time distribution. Bold indicates significance.

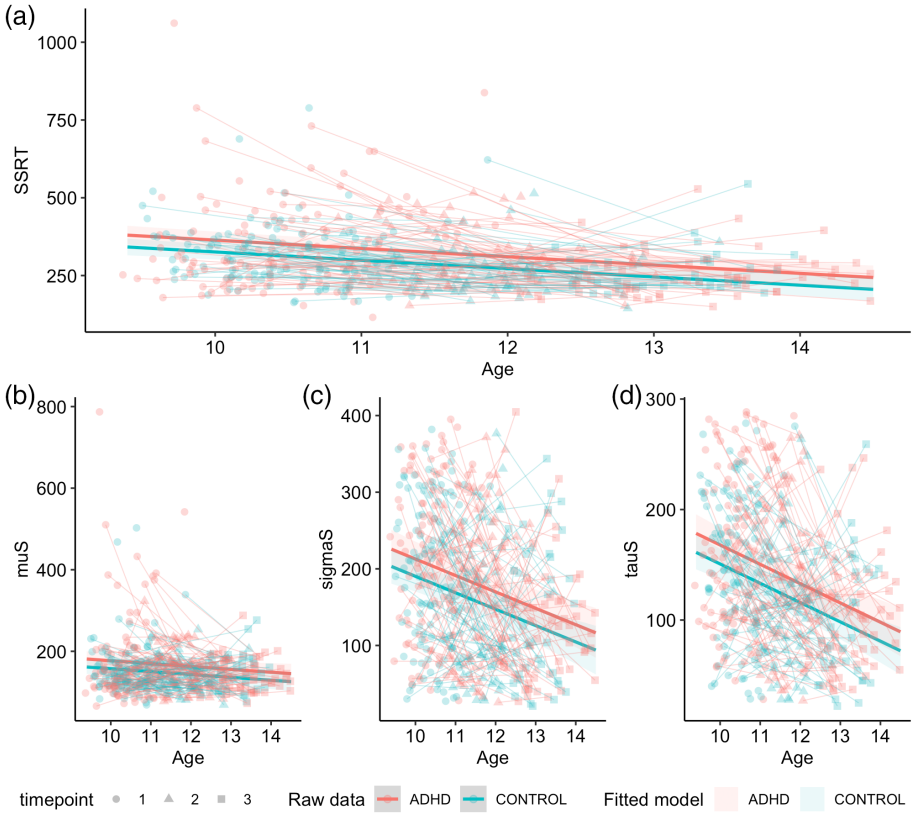

FIGURE 3 Best-fitting group-main effect models for stop trial parameters. A: SSRT; B: muS; C: sigmaS; D: tauS. Age in years; SSRT, muS, sigmaS, tauS in ms.

3.2 | Developmental trajectories of fronto-basal-ganglia WM

3.2.1 | Left-hemisphere fronto-basal-ganglia circuit

Model comparisons revealed significant age-related maturation in FC (log) across the left hemispheric IFG-preSMA and preSMA-STN pathways (Figure 5a,b; Table 6; also see Tables S14–S19 of Supporting Information B). The inclusion of a main effect of group did not significantly improve model fit, indicating that ADHD and non-ADHD children did not significantly differ in WM morphology. Whilst we identified a significant age-effect for the left IFG-STN pathway with respect to FC (log), these effects disappeared after applying FDR correction (Figure 5c). When looking at the best fitting model for FC (log) in the left IFG-preSMA pathway, we found that sex, total brain volume (eTIV) and scanner type significantly predicted changes in fibre morphology, whilst a trend towards significance was observed for SES. In contrast, mean head motion (mean FWD) and medication status were not significant predictors. Evaluation of the best-fitting model for FC (log) in the left preSMA-STN pathway demonstrated a

TABLE 4 Parametric and smooth terms for the best-fitting models for the stop trial parameters.

	SSRT			muS	sigmaS			tauS		
Parametric coefficients	***Est.(SE)***	***t***	***p***	***Est.(SE)***	***t***	***p***	***Est.(SE)***	***t***	***p***	***Est.(SE)***	***t***	***p***
Intercept	326.11 (12.81)	25.46	**<.001**	166.94 (7.77)	21.50	**<.001**	182.51 (10.45)	17.47	**<.001**	143.26 (7.33)	19.54	**<.001**
Group	−38.00 (12.79)	−2.97	**<.001**	−19.57 (7.75)	−2.52	**0.01**	−22.51 (10.43)	−2.16	**0.03**	−17.16 (7.32)	−2.34	**.02**
SES_c	−0.27 (0.14)	−1.88	.06	−0.12 (0.09)	−1.37	0.17	−0.04 (0.12)	−0.32	.75	−0.15 (0.08)	−1.80	.07
med	−32.21 (17.78)	−1.81	.07	−17.88 (10.84)	−1.65	0.10	−22.45 (14.58)	−1.54	.12	−13.64 (10.19)	−1.34	.18
Sex	7.97 (12.67)	0.63	.53	−0.41 (7.68)	−0.05	0.96	13.20 (10.34)	1.28	.20	7.12 (7.12)	0.98	.33
Smooth terms	***Edf (Ref.df)***	***F***	***p***	***Edf (Ref.df)***	***F***	***p***	***Edf (Ref.df)***	***F***	***p***	***Edf (Ref.df)***	***F***	***p***
s(age_c)	1.00 (1.00)	34.50	**<.001**	1.00 (1.00)	5.57	**0.02**	1.01 (1.01)	28.84	**<.001**	1.00 (1.00)	44.22	**<.001**
s(SID)	76.74 (255.00)	0.45	**<.001**	30.70 (255.00)	0.14	0.11	39.19 (255.00)	0.19	**0.04**	71.94 (255.00)	0.41	**<.001**

Note: Est.: estimated regression parameter; SE: standard error; edf: estimated degrees of freedom; Ref.df: reference degrees of freedom; group: ADHD and controls; SES_c: mean-centred SES; med: medication status; sex: males and females; s(age_c): smoothed mean-centred age; s(SID): subject ID entered as a random effect. SSRT: stop-signal reaction time; muS: Mu of the stop-signal reaction time distribution; sigmaS: Sigma of the stop-signal reaction time distribution; tauS: Tau of the stop-signal reaction time distribution. Bold indicates significance.

significant effect of eTIV and scanner type on changes in fibre morphology, whilst SES, sex, and mean FWD were not significant. Further, no models were a significant improvement from the null for FD in all tracts of interest in the left hemisphere.

3.2.2 | Right-hemisphere fronto-basal-ganglia circuit

Results for the right hemispheric tracts revealed a significant age effect for FC (log) in all three tracts of interest: (1) IFG-preSMA, (2) IFG-STN, and (3) preSMA-STN (Figure 5d–f; Table 7). Inclusion of a main effect of group did not significantly improve model fit. Evaluations of the best-fitting models found that eTIV and scanner type were significant predictors of change in fibre morphology across all tracts-of-interest. We also observed best-fitting age-models for FD in the right IFG-STN and preSMA-STN pathways, whereby FD increased with age, but these effects disappeared after FDR correction. See Tables S20–S25 of Supporting Information B.

3.3 | Predicting change in response inhibition from change in fronto-basal-ganglia WM

Extending the best-fitting behavioural models from Section 3.1, the addition of age-related changes in FC (log) in the bilateral IFG-preSMA, preSMA-STN, and right hemispheric IFG-STN pathways revealed a significant main effect of FC (log) slope underlying the left IFG-preSMA pathway with respect to the skew of the stopping distribution (tauS). We also observed a significant interaction effect between FC (log) underlying the left preSMA-STN pathway and age with respect to the within-subject variability in responses to the correct stimulus on go trials (sigma.true). In the right hemisphere, a significant main effect was also identified for FC (log) in relation to tauS within the right IFG-STN pathway. In contrast, the addition of age-related changes in FC (log) in the abovementioned tracts of interest did not significantly improve the best-fitting models for all other SST measures. Statistical information for all best-fitting models can be accessed in Table 8. All model comparisons are presented in Tables S26–S30 of Supporting Information B.

4 | DISCUSSION

The present study was the first to examine the developmental trajectory of SST performance and its relationship to fronto-basal-ganglia WM organisation in a sample of ADHD and non-ADHD children. Using the parametric race model, we demonstrate evidence of SST performance deficits in ADHD being driven by increased variability and skewness of the go-and-stop trial distributions. Children with ADHD also committed more trigger-and-go failures than children without ADHD, supporting previous accounts for the potential role of attentional impairments in poor SST performance. Our analysis

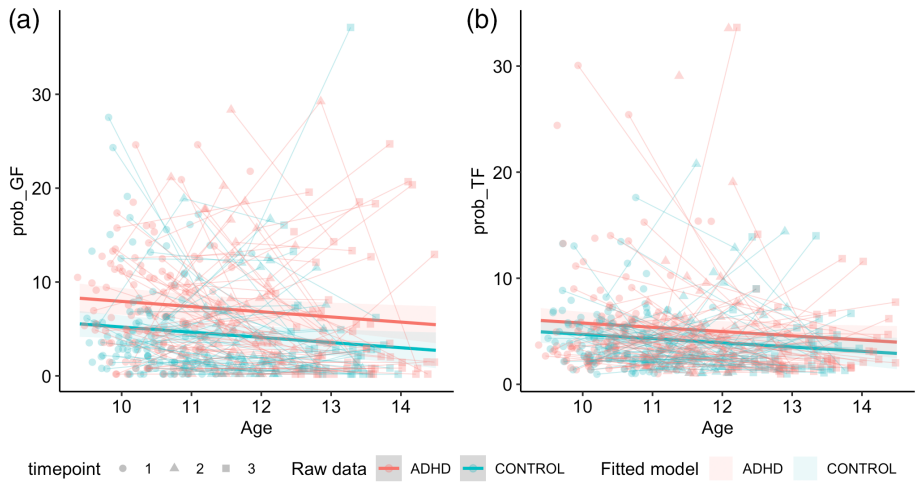

FIGURE 4 Best-fitting group main-effect models for attention-based parameters. A: prob_GF; B: prob_TF. Age in years; prob_GF and prob_TF in percentage (%).

TABLE 5 Parametric and smooth terms for the best-fitting models for task-failure parameters.

	Prob_GF			Prob_TF		
Parametric coefficients	***Est.(SE)***	***t***	***p***	***Est.(SE)***	***t***	***p***
Intercept	7.16 (0.66)	10.76	**<.001**	5.21 (0.48)	10.83	**<.001**
Group	−2.73 (0.66)	−4.11	**<.001**	−1.06 (0.48)	−2.22	**.03**
SES_c	−0.01 (0.01)	−1.43	.16	−0.01 (0.01)	−1.54	.12
med	−1.11 (0.92)	−1.20	.23	−0.74 (0.67)	−1.10	.27
Sex	−0.03 (0.66)	−0.05	.96	0.17 (0.48)	0.35	.73
Smooth terms	***Edf (Ref.df)***	***F***	***p***	***Edf (Ref.df)***	***F***	***p***
s(age_c)	1.00 (1.01)	5.68	**.02**	1.00 (1.00)	4.53	**.03**
s(SID)	86.60 (255.00)	0.59	**<.001**	20.83 (255.00)	0.09	.17

Note: Parametric and smooth terms for the best-fitting models for task-failure parameters. Est.: Estimated regression parameter; SE: standard error; edf: estimated degrees of freedom; Ref.df: reference degrees of freedom; group: ADHD & controls; SES_c: mean-centred SES; med: medication status; sex: Males & Females; s(age_c): smoothed mean-centred age; s(SID): subject ID entered as a random effect. Prob_GF: probability of go failures; Prob_TF: probability of trigger failures. Bold indicates significance.

looking at WM maturation within the fronto-basal-ganglia circuit revealed no group differences in age-related increases in fibre cross-section. Finally, our brain-behavioural models revealed that age-related changes in fibre cross-section were associated with reduced within-subject variability and skewness in the stop-trial and correct go-trial responses across both ADHD and non-ADHD children. Taken together, the latter results suggest that although fronto-basal-ganglia circuit WM development may be implicated in general improvements in SST performance, alterations within this circuit do not appear to be associated with ADHD-related inhibitory deficits. Implications of the present findings are discussed in detail below.

4.1 | The role of attentional failures in ADHD-related inhibitory deficits

Consistent with the vast behavioural literature on ADHD-related SST performance deficits, our study found evidence of longer SSRTs in the ADHD group compared to non-ADHD controls (Alderson et al., 2007; Lijffijt et al., 2005; Lipszyc & Schachar, 2010). Our parametric modelling approach using the EXG3 framework (Matzke et al., 2019) revealed that in addition to having prolonged mean SSRT (mu), children with ADHD were more variable (sigma) and had increased skewness in the RT distribution (tau) during stop trials across the transition to adolescence. These effects were not limited to stop trials. Whilst both groups displayed similar age-related improvements in overall go trial RT and in the mean of the correct go response (mu.true), the ADHD group showed higher within-subject performance variability than non-ADHD controls when responding to the correct stimulus on go trials (sigma.true). Increased sigma in children with ADHD reflects more inconsistent performance during the task. Likewise, increased tau suggests that children with ADHD are more likely to engage in more frequent abnormally slow responses compared to their neurotypical counterparts (Karalunas & Huang-Pollock, 2013; Kofler et al., 2013; Weigard et al., 2019). These findings may perhaps be interpreted as that of ADHD individuals engaging in higher probability of proactive control behaviours compared to non-ADHD participants. Specifically, individuals with ADHD often show increased slowing of

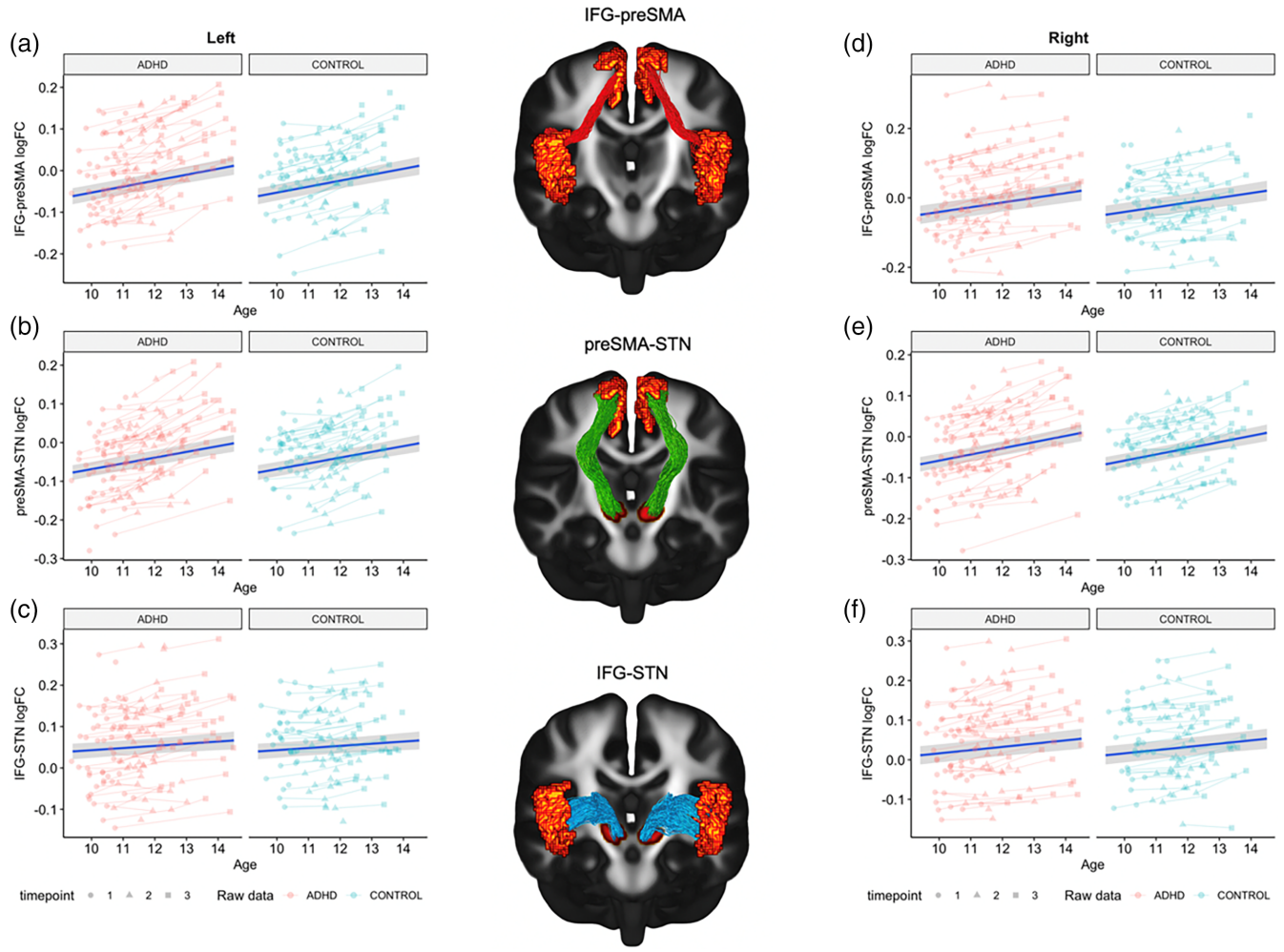

FIGURE 5 Spaghetti plots for the best fitting models of the fronto-basal-ganglia circuit. (a) Left IFG-preSMA; (b) Left preSMA-STN; (c) Left IFG-STN; (d) Right IFG-preSMA; (e) Right preSMA-STN; (f) Right IFG-STN. Age in years.

TABLE 6 Parametric and smooth terms for the best-fitting models for left fronto-basal-ganglia circuit.

	Left IFG-preSMA FC (log)			Left preSMA-STN FC (log)		
Parametric coefficients	***Est.(SE)***	***t***	p_{FDR}	***Est.(SE)***	***t***	p_{FDR}
Intercept	0.001 (0.010)	0.059	.995	−0.004 (0.010)	−0.393	.820
SES_c	0.000 (0.000)	2.309	.068	0.000 (0.000)	1.890	.144
Sex	0.040 (0.012)	3.260	**.006**	0.024 (0.012)	1.997	.119
meanFWD_c	0.000 (0.007)	0.009	.995	0.004 (0.007)	0.560	.714
eTIV_c	0.000 (0.000)	6.166	**<.001**	0.000 (0.000)	7.110	**<.001**
Scanner	−0.030 (0.004)	−7.249	**<.001**	−0.040 (0.004)	−9.185	**<.001**
med	0.001 (0.008)	0.108	.994	−0.001 (0.008)	−0.182	.963
Smooth terms	***Edf (Ref.df)***	***F***	p_{FDR}	***Edf (Ref.df)***	***F***	p_{FDR}
s(age_c)	1.000 (1.000)	84.085	**<.001**	1.000 (1.000)	80.403	**<.001**
s(SID)	139.517 (144.000)	50.172	**<.001**	138.908 (144.000)	38.987	**<.001**

Note: Est.: estimated regression parameter; SE: standard error; edf: estimated degrees of freedom; Ref.df: reference degrees of freedom; p_{FDR}: false discovery rate corrected *p* value; s(age_c): smoothed mean-centred age; SES_c: mean-centred SES; med: medication status; sex: Males & Females; s(SID): subject ID entered as a random effect; meanFWD_c: mean-centred mean FWD; eTIV_c: mean-centred eTIV; scanner: ordered factor of scanner type. Bold indicates significance.

TABLE 7 Parametric and smooth terms for the best-fitting models for right fronto-basal-ganglia circuit.

	Right IFG-preSMA FC (log)			Right IFG-STN FC (log)			Right preSMA-STN FC (log)		
Parametric coefficients	***Est.(SE)***	***t***	p_{FDR}	***Est.(SE)***	***t***	p_{FDR}	***Est.(SE)***	***t***	p_{FDR}
Intercept	−0.006 (0.014)	−0.471	.769	0.042 (0.012)	3.523	**.003**	−0.010 (0.009)	−1.033	.513
SES_c	0.000 (0.000)	1.828	.159	0.000 (0.000)	2.285	.071	0.000 (0.000)	1.196	.433
Sex	0.033 (0.017)	1.949	.129	0.030 (0.015)	2.019	.116	0.017 (0.011)	1.514	.274
meanFWD_c	0.001 (0.007)	0.188	.963	0.007 (0.007)	1.044	.512	−0.006 (0.007)	−0.906	.572
eTIV_c	0.000 (0.000)	4.108	**<.001**	0.000 (0.000)	6.704	**<.001**	0.000 (0.000)	8.760	**<.001**
Scanner	−0.012 (0.005)	−2.572	**.039**	−0.012 (0.004)	−2.943	**.015**	−0.024 (0.004)	−5.526	**<.001**
med	0.004 (0.009)	0.410	.814	0.010 (0.008)	1.189	.433	0.001 (0.008)	0.163	.968
Smooth terms	***Edf (Ref.df)***	***F***	p_{FDR}	***Edf (Ref.df)***	***F***	p_{FDR}	***Edf (Ref.df)***	***F***	p_{FDR}
s(age_c)	1.000 (1.000)	61.693	**<.001**	1.001 (1.001)	26.755	**<.001**	1.000 (1.000)	85.893	**<.001**
s(SID)	140.984 (144.000)	77.192	**<.001**	140.738 (144.000)	72.992	**<.001**	138.272 (144.000)	34.728	**<.001**

Note: Est.: estimated regression parameter; SE: standard error; edf: estimated degrees of freedom; Ref.df: reference degrees of freedom; p_{FDR}: false discovery rate corrected *p* value; s(age_c): smoothed mean-centred age; SES_c: mean-centred SES; med: medication status; sex: Males & Females; s(SID): subject ID entered as a random effect; meanFWD_c: mean-centred mean FWD; eTIV_c: mean-centred eTIV; scanner: ordered factor of scanner type. Bold indicates significance.

TABLE 8 Parametric and smooth terms for the best-fitting brain-behavioural models.

	Left preSMA-STN and sigma.true			Left IFG-preSMA and tauS			Right IFG-STN and tauS		
Parametric coefficients	***Est. (SE)***	***t***	***p***	***Est. (SE)***	***t***	***p***	***Est. (SE)***	***t***	***p***
Intercept	123.58 (11.11)	11.10	**<.001**	124.58 (13.58)	9.17	**<.001**	129.40 (13.48)	9.60	**<.001**
FC (log) slope	−20.33 (2840.20)	−0.01	.99	7189.68 (3419.69)	2.10	**.04**	−4684.68 (2273.08)	−2.06	**.04**
SES_c	−0.12 (0.09)	−1.28	.20	−0.27 (0.10)	−2.65	**.01**	−0.20 (0.10)	−1.89	.06
Group	−19.42 (8.09)	−2.40	**.02**	−12.58 (9.01)	−1.40	.16	−16.20 (9.22)	−1.76	.08
med	−2.27 (10.85)	−0.21	.83	−22.02 (12.29)	−1.79	.07	−23.20 (12.55)	−1.85	.07
Sex	11.35 (8.14)	1.39	.16	3.24 (9.12)	0.36	.72	9.76 (9.30)	1.05	.30
Scanner	6.09 (10.34)	0.59	.56	15.56 (14.01)	1.11	.27	5.86 (13.51)	0.43	.66
Smooth terms	***Edf (Ref.df)***	***F***	***p***	***Edf (Ref.df)***	***F***	***p***	***Edf (Ref.df)***	***F***	***p***
s(age_c)	1.00 (1.00)	7.20	**.01**	1.66 (2.01)	5.37	**.01**	1.34 (1.58)	5.22	**.01**
age_c × FC (log) slope	1.68 (1.99)	5.72	**.01**	–	–	–	–	–	–
s(SID)	66.23 (142.00)	1.00	**<.01**	36.51 (142.00)	0.36	**.02**	45.27 (142.00)	0.49	**<.001**

Note: Est.: estimated regression parameter; SE: standard error; edf: estimated degrees of freedom; Ref.df: reference degrees of freedom; *p*: *p* value; FC (log) slope: slope of FC; s(age_c): smoothed mean-centred age; SES_c: mean-centred SES; med: medication status; sex: Males and Females; s(SID): subject ID entered as a random effect; scanner: ordered factor of scanner type; age_c × FC (log) slope: age × FC (log) slope interaction. Bold indicates significance.

responses following error trials (post-error slowing; Balogh & Czobor, 2016). Alternatively, increased variability and skewness of RT distributions may also be indicative of greater inconsistencies in task-related performance (commonly termed inter-individual variability; IIV), a phenomenon ubiquitous to this specific neurodevelopmental population (Halliday et al., 2021; Kofler et al., 2013; Salum et al., 2019). This idea of ADHD being associated with more inconsistent task performance is not a new phenomenon (De Zeeuw et al., 2008; Klein et al., 2006; Uebel et al., 2010). Indeed, a 2013 meta-analysis of 319 studies demonstrated that ADHD-diagnosed individuals tended to have more variable performance than that of neurotypical controls across a range of cognitive tasks (Kofler et al., 2013). Perhaps most strikingly, Kofler and colleagues demonstrated that group effects of poorer performance were ameliorated after controlling for RT variability, further lending support for IIV as a significant behavioural phenotype in this disorder.

In addition to being more variable on go and stop trials, children with ADHD also displayed a greater probability of engaging in trigger (i.e., responding on stop-signal trials) and go failures (i.e., omissions on go trials) across age compared to non-ADHD controls. In the context of the race model, higher probability of engaging in trigger and go failures likely reflects lapses in attention with respect to stimulus detection or difficulties with vigilance to task-relevant stimuli (Logan & Cowan, 1984; Matzke, Hughes, et al., 2017; Matzke et al., 2019; Weigard et al., 2019). This is consistent with evidence of ADHD-children showing marked impairments in error-processing and

performance adjustment in response to changing task demands (Karalunas & Huang-Pollock, 2013; Shiels et al., 2012). Furthermore, the application of the parametric race model in a longitudinal sample demonstrated, for the first time, that these deficits are consistent across the transition from childhood to adolescence. These effects were robust after adjusting for medication status and SES, suggesting that aberrant performance on the SST is a stable behavioural phenotype in childhood ADHD. It is also important to note that performance on the SST for both children with and without ADHD improved with age, supporting previous longitudinal studies of a general improvement in executive functioning from childhood to adolescence (Curley et al., 2018; Madsen et al., 2020; Singh et al., 2022; Williams et al., 1999).

Together with the cross-sectional findings of Weigard et al. (2019), the results of the present work further support the growing consensus that ADHD-related SST performance deficits may be the consequence of impairments in attentional-based processes that affect the fidelity and consistency of stopping performance. Recent neurophysiological models of response inhibition posit that successful stopping is concomitant with a range of peripheral cognitive mechanisms, such as stimulus detection and attentional monitoring (Diesburg & Wessel, 2021; Jana et al., 2020; Skippen, 2019). In the classic SST, stop-signals occur on a subset of trials to ensure that the go response is the default behaviour (Verbruggen, 2019). Given this design characteristic, the outcome of response inhibition during the SST is invariably confounded by the reliability to which the individual can successfully detect and attend to the signal. Here, the observed performance differences in the SST are not necessarily the result of inefficient inhibitory mechanisms, but rather a failure to successfully engage in attentional mechanisms that allow for more consistent on-task performance. Nonetheless, traditional methods of quantifying SSRT often use summary measures (i.e., the mean) which cannot account for these features in the data, leading to potentially erroneous interpretations of performance differences in the SST (Matzke et al., 2013; Matzke, Hughes, et al., 2017).

Thus, our findings of ADHD-related increases in trigger and go failures highlight the importance of considering these other perceptual and attentional processes that affect motor inhibition. These results have important ramifications when understanding of ADHD as a disorder of inhibition. Given that attentional difficulties are one of the hallmark features of ADHD, future work should investigate the degree to which other behavioural symptoms in ADHD that have previously been thought to be driven by inhibition problems (i.e., hyperactivity/impulsivity) might be in fact attributable, at least in part to deregulated attention. Clarifying the distinction between deficits in attention and overt-stopping performance also has important clinical implications for the ongoing development of targeted intervention strategies in ADHD. Specifically, interventions directed towards improving top-down attentional and vigilance systems may be more effective in improving inhibitory control deficits and its associated corollaries, than interventions solely directed at improving behavioural stopping. In sum, our behavioural findings underscore the argument that ADHD-related performance deficits in the SST are not solely due to modular deficits in stopping behaviour, but rather in more general cognitive processes that influence performance across tasks (i.e., attention).

4.2 | Fronto-basal-ganglia WM maturation and associations with response inhibition in typical and atypical development

The transition to adolescence is marked by extensive reorganisation of structural connections within the brain, which in turn, correspond to rapid gains in higher-order cognitive functions (Goddings et al., 2021). Therefore, the next major aim of this study was to explore whether the observed age-related deficits in SST performance in children with ADHD are associated with altered developmental trajectories of fronto-basal-ganglia WM organisation. In contrast to our hypothesis, our neuroimaging models found no evidence of disrupted fronto-basal-ganglia WM development in children with ADHD. More specifically, both groups displayed comparable age-related increases in fibre cross-section (FC (log)) across the bilateral IFG-preSMA, preSMA-STN and right IFG-STN pathways. Further, both ADHD and non-ADHD children demonstrated similar trajectories for associations between age-changes in FC (log) and SST performance. Our brain-behavioural models revealed that developmental reductions in the propensity of engaging in extreme responses during stop trials (tau) were driven by greater change in FC (log) of the left IFG-preSMA and right IFG-STN pathways. We also observed a significant age-by-FC (log) interaction in the left preSMA-STN with respect to reductions in variability in correct responses to go trials (sigma.true). Taken together, while WM maturation within fronto-basal-ganglia circuitry may contribute to age-related changes in SST performance, this effect does not differ between ADHD and non-ADHD children.

Recent longitudinal FBA studies have observed altered white matter profiles across several frontal, striatal and associative tracts (Damatac et al., 2020; Fuelscher et al., 2021; Hyde et al., 2021), which may provide evidence for a maturational lag in brain development in ADHD (El-Sayed et al., 2003; Shaw, 2007; Sripada et al., 2014). Returning to our results, the lack of significant group differences may point to a possible 'normalization' of these pathways in ADHD to levels similar to neurotypical children during later childhood and into adolescence. This is supported by previous longitudinal studies examining the developmental trajectories of grey matter in children with ADHD have demonstrated that the remittance of ADHD symptomatology can be explained by a convergence of neural features from atypical baseline levels toward more typical brain structure in adolescence and adulthood (i.e., the 'convergence model'; Shaw, 2013). Hence, it is possible that any arrested developmental processes in relation to fronto-basal-ganglia WM in ADHD might have already been resolved at earlier developmental stages, leading to similar developmental trajectories during early-to-mid adolescence. However, these claims are speculative at best and future work is warranted to explore these questions. Together with our behavioural findings, our results suggest that whilst children with ADHD show consistent

deficits in SST performance across this age-span, they show comparable trajectories of fronto-basal-ganglia WM development.

The lack of significant group effects, whilst contrary to our hypothesis, is aligned with previous nonsignificant cross-sectional findings in relation to associations between WM organisation and ADHD-related SST performance (Albajara Senz et al., 2020; Bessette & Stevens, 2019; Tremblay et al., 2020). However, the current study was the first to directly test this relationship in the fronto-basal-ganglia circuit, a network that has been well established in healthy individuals to be critical for inhibitory control (Aron, Durston, et al., 2007; Aron, Behrens, et al., 2007). In lieu of these findings, this has important ramifications about the pathophysiology of ADHD as it is possible that the observed functional deficits of poor SST performance outcomes in ADHD (as seen in the results of the parametric race model analyses) are independent of the structural integrity of this core inhibitory control network. Instead, the mechanisms underpinning ADHD-related inhibitory deficits (as seen in our behavioural models) may lie elsewhere. A recent meta-analysis by Zhang et al. (2017) of 225 fMRI studies assessing the neural substrates of response inhibition established that an extensive spatially distributed neural system comprising frontostriatal and ventral–attentional networks subserves inhibitory control. The distributed nature of the ventral attention and frontostriatal networks at subserving a range of cognitive functions would suggest that white matter tracts underlying these networks may also contribute to inter-individual differences in other cognitive processes involved in the inhibitory response (i.e., attention, stimulus detection) (Boen et al., 2021; Luna et al., 2021; Thomson et al., 2022a). As such, future work should consider the maturation of these alternative networks in explaining the development of response inhibition during childhood and the degree to which the maturational profiles of these alternative networks differ in children with ADHD. To this end, by incorporating these other networks together with the parameters derived from the parametric race model, we would be better able to disentangle the neurostructural correlates that underpin these specific processes on overall response inhibitory performance.

Age-related increases in FC (log) may be driven by increased myelination or enlargement of the extracellular space between fibre bundles during development (Genc et al., 2018, 2020). In the context of the FBA framework, increased tract morphology may likely facilitate more efficient neural communication between brain regions (Genc et al., 2018). Thus, our findings demonstrate that greater maturation of fronto-basal-ganglia tract morphology may improve the functional integrity this circuit, leading to better task-based performance at later developmental ages by way of reduced variability and fewer extreme responses. At a broad level, these findings corroborate indirect DTI-based evidence of associations between increased white matter tract organisation and more consistent performance across a range of cognitive paradigms (Fjell et al., 2011; Tamnes et al., 2012). For example, a study by Tamnes et al. (2012) found that increased within-subject variability in the speed of correct responses on a Flanker Task was associated with reductions in FA, MD and RD within the corticospinal tract, the left superior longitudinal fasciculus, the uncinate fasciculus, the forceps minor, and in the genu and splenium of the corpus callosum.

In contrast, we did not find any significant age effects for fronto-basal-ganglia fibre density (FD). Prior studies in typically developing children report that FD increases during childhood (Genc et al., 2018). Given that no such effects reached significance in the current study, these findings may indicate that microstructure within the fronto-basal-ganglia circuit does not mature dramatically during the transition to adolescence. Alternatively, it is possible at such effects may be subtle. This mirrors our previous study in typically developing children, suggesting that the development of fronto-basal-ganglia WM is uniquely localized to large-scale morphological changes, rather than microstructure (Singh et al., 2022).

4.3 | Strengths, limitations and future directions

Strengths of this study include the use of more specific measures to quantify the development of response inhibition and fronto-basal-ganglia WM. The FBA framework is robust to intra-voxel changes in fibre orientation (Dhollander et al., 2021; Raffelt et al., 2017), thus providing a more biologically specific approach with which to quantify changes in WM properties compared to tensor-based models. Further, the parametric race model provides a multivariate framework for quantifying intraindividual changes in RT distribution for go and stop trials, whilst simultaneously accounting for attention-based contaminants (Matzke, Love, & Heathcote, 2017; Matzke et al., 2019). Nevertheless, some limitations of the present work must be considered. Previous work by Matzke, Love, and Heathcote (2017) demonstrated poorer parameter recovery in datasets containing lower numbers of stop-trials. Hence, while it is possible that the low number of stop-trials in the current study (48 trials) may have impacted upon the reliability of our parameter estimates, the STOP-IT paradigm (Verbruggen et al., 2008) is arguably the most popular variant of the SST to date, and largely conforms to best-practice guidelines for the administration of the SST (Verbruggen, 2019). While increasing the number of stop-trials does improve validity, we must be mindful of the feasibility of doing so in experimental studies of clinical populations, especially in children or those characterised by deficits of attention (such as ADHD). Increasing trial numbers in these cases may encourage poor task adherence and introduce additional confounds in subsequent estimation of SST performance. As such, future studies aiming to replicate these effects must strike a balance between feasibility and validity.

In addition, ADHD is a heterogeneous disorder, and therefore, the extent to which inhibitory deficits are expressed may differ between symptom profiles. Due to the limited number of participants across the three timepoints, we were not able to conduct subgroup analyses considering the differential effects of ADHD presentation (e.g., primarily inattentive, or hyperactive) on age-related trajectories of response inhibition and fronto-basal-ganglia WM. Furthermore, as results from the current study are taken from a population-based sample, the observed effects may differ to clinical cohorts, which are characterized by more severe symptoms. Hence, future work should seek to replicate the current findings across different ADHD subtypes to

see if these trajectories are a consistent phenotype. Finally, we note that our study was impacted by relatively high attrition rates, resulting in an unbalanced dataset across the three timepoints. Furthermore, our attrition analysis on a subset of participants revealed significant differences in SST performance in the ADHD group who had completed one, two or all three timepoints for both behavioural and imaging samples (See Supporting Information). Hence, it is possible that the high attrition rates in our study may have impacted our power at detecting significant group effects in our neuroimaging and brain-behavioural models. Given that this study utilised a pre-collected sample, the ability to control for any attrition-related biases are minimal. Hence, we cannot rule out any effects that this may have on our main findings. Furthermore, it is important to acknowledge that there has been much discussion around the need for large sample sizes to robustly investigate brain-behavioural relationships (see Marek et al., 2022). Whilst we recommend that future studies should consider replicating these findings in larger cohorts to ascertain the robustness of these effects, we note that the current study adopted an a priori tract of interest approach along with tract-averaged values of fixelwise metrics to reduce the number of comparisons in our analysis of brain-behavioural effects. Nevertheless, it must be noted that the use of tract averaged values limits the ability to identify fixel-specific associations in WM organisation to phenotypical outcomes. However, since the completion of the present study, newer methods such as ModelArray (Zhao et al., 2023) have been developed that allows for the application of advanced mixed modelling of fixel-level data in repeated-measures cohorts (albeit without using cluster-based CFE), thus providing a promising alternative for future work to further identify the role of WM neurodevelopment in response inhibition across healthy and clinical populations.

5 | CONCLUSION

We identified consistent deficits in SST performance in the ADHD group relative to controls. By using the parametric race model, we observed that children with ADHD not only had higher within-subject variability and extreme responding on the SST, but also engaged in more task-related failures across the age-span (i.e., trigger and go failures) compared to non-ADHD controls, thus highlighting the potentially important contribution of attentional mechanisms on the efficacy of stopping performance. In contrast, no group differences emerged for the development of fronto-basal-ganglia WM, with both ADHD and non-ADHD children demonstrating similar age-related increases in FC (log) within selected tracts of the circuit. Finally, both ADHD and non-ADHD children showed similar trajectories in the relationship between fronto-basal-ganglia circuit maturation and reductions in the skewness of the stop trial distribution and variability in correct go trials.

AUTHOR CONTRIBUTIONS

Mervyn Singh: Conceptualization; methodology; formal analysis; writing—original draft; writing—review and editing. **Patrick Skippen:** Methodology; formal analysis; writing—review and editing. **Jason He:** Methodology; writing—review and editing. **Phoebe Thomson:** Methodology; formal analysis; writing—review and editing. **Ian Fuelscher:** Supervision; conceptualization; methodology; writing—original draft; writing—review and editing. **Karen Caeyenberghs:** Writing—review and editing. **Vicki Anderson:** Writing—review and editing. **Christian Hyde:** Supervision; conceptualization; methodology; writing—original draft; writing—review and editing. **Timothy J. Silk:** Supervision; conceptualization; project administration; funding acquisition; methodology; writing—original draft; writing—review and editing.

ACKNOWLEDGEMENTS

We thank the Australian Government National Computational Merit Allocation Scheme for the provision of computational resources through the Monash M3 Cluster. We are grateful to the Royal Children's Hospital medical staff and researchers at the Murdoch's Children Research Institute for their involvement in the collection of MRI and behavioural data for this project. We also thank Dr Nandi Vijayakumar (N.V.), Ms. Lillian Dipnall (L.D.), and Dr. Shania Soman (S.S.) for their assistance in quality assessing the pre-processed diffusion MRI images. Finally, we thank the parents, guardians and children who took part in this study. Open access publishing facilitated by Deakin University, as part of the Wiley - Deakin University agreement via the Council of Australian University Librarians.

FUNDING INFORMATION

NICAP was funded by the National Health and Medical Research Council of Australia (NHMRC; project grant #1065895). Ethics approval was granted by the Royal Children's Hospital Human Research Ethics Committee, Melbourne (#34071) and ratified by the Deakin University Human Research Ethics Office (#2016-394). Mervyn Singh is supported by a Postgraduate Research Scholarship from Deakin University.

CONFLICT OF INTEREST STATEMENT

The authors declare no conflicts of interest.

DATA AVAILABILITY STATEMENT

Data from the Children's Attention Project cohort are available via Lifecourse: https://lifecourse.melbournechildrens.com/cohorts/cap-nicap/. Due to ethical guidelines, raw participant data cannot be made publicly available. However, de-identified data can be shared upon reasonable request. Analysis code for this study is accessible via: https://github.com/MervSingh/Longitudinal_SST_FBA_ADHD.git.

ORCID

Mervyn Singh https://orcid.org/0000-0001-8058-3995
Christian Hyde https://orcid.org/0000-0003-4833-4782

REFERENCES

Albajara Senz, A., Villemonteix, T., Slama, H., Baijot, S., Mary, A., Balriaux, D., Metens, T., Kavec, M., Peigneux, P., & Massat, I. (2020). Relationship between white matter abnormalities and neuropsychological measures in children with ADHD. *Journal of Attention Disorders*, *24*, 1020–1031.

Alderson, R. M., Rapport, M. D., & Kofler, M. J. (2007). Attention-deficit/hyperactivity disorder and behavioral inhibition: A meta-analytic review of the stop-signal paradigm. *Journal of Abnormal Child Psychology*, *35*, 745–758.

Alderson, R. M., Rapport, M. D., Sarver, D. E., & Kofler, M. J. (2008). ADHD and behavioral inhibition: A re-examination of the stop-signal task. *Journal of Abnormal Child Psychology*, *36*, 989–998.

American Psychiatric Association. (2013). *Diagnostic and statistical manual of mental disorders* (5th ed.). American Psychiatric Publishing.

Andersson, J. L. R., & Sotiropoulos, S. N. (2016). An integrated approach to correction for off-resonance effects and subject movement in diffusion MR imaging. *NeuroImage*, *125*, 1063–1078.

Andersson, J. L. R., Graham, M. S., Drobnjak, I., Zhang, H., Filippini, N., & Bastiani, M. (2017). Towards a comprehensive framework for movement and distortion correction of diffusion MR images: Within volume movement. *NeuroImage*, *152*, 450–466.

Andersson, J. L. R., Graham, M. S., Zsoldos, E., & Sotiropoulos, S. N. (2016). Incorporating outlier detection and replacement into a non-parametric framework for movement and distortion correction of diffusion MR images. *NeuroImage*, *141*, 556–572.

Andersson, J. L. R., Skare, S., & Ashburner, J. (2003). How to correct susceptibility distortions in spin-echo echo-planar images: Application to diffusion tensor imaging. *NeuroImage*, *20*, 870–888.

Annis, J., & Palmeri, T. J. (2018). Bayesian statistical approaches to evaluating cognitive models: Bayesian statistical approaches. *Wiley Interdisciplinary Reviews: Cognitive Science*, *9*, e1458.

Aoki, Y., Cortese, S., & Castellanos, F. X. (2018). Research review: Diffusion tensor imaging studies of attention-deficit/hyperactivity disorder: Meta-analyses and reflections on head motion. *Journal of Child Psychology and Psychiatry*, *59*, 193–202.

Aron, A. R., Behrens, T. E., Smith, S., Frank, M. J., & Poldrack, R. A. (2007). Triangulating a cognitive control network using diffusion-weighted magnetic resonance imaging (MRI) and functional MRI. *The Journal of Neuroscience*, *27*, 3743–3752.

Aron, A. R., Durston, S., Eagle, D. M., Logan, G. D., Stinear, C. M., & Stuphorn, V. (2007). Converging evidence for a fronto-basal-ganglia network for inhibitory control of action and cognition. *Journal of Neuroscience*, *27*, 11860–11864.

Australian Bureau of Statistics. (2013). Census of population and housing: socio-economicindexes for areas (SEIFA), Australia, 2011. cat. no. 2033.0. 55.001 https://www.abs.gov.au/ausstats/abs@.nsf/DetailsPage/2033.0.55.0012011. ABS, Canberra

Ball, G., Malpas, C. B., Genc, S., Efron, D., Sciberras, E., Anderson, V., Nicholson, J. M., & Silk, T. J. (2019). Multimodal structural neuroimaging markers of brain development and ADHD symptoms. *The American Journal of Psychiatry*, *176*, 57–66.

Balogh, L., & Czobor, P. (2016). Post-error slowing in patients with ADHD: A meta-analysis. *Journal of Attention Disorders*, *20*, 1004–1016.

Band, G. P. H., van der Molen, M. W., & Logan, G. D. (2003). Horse-race model simulations of the stop-signal procedure. *Acta Psychologica*, *112*, 105–142.

Barkley, R. A. (1997). Behavioral inhibition, sustained attention, and executive functions: Constructing a unifying theory of ADHD. *Psychological Bulletin*, *121*, 65–94.

Baum, G. L., Roalf, D. R., Cook, P. A., Ciric, R., Rosen, A. F. G., Xia, C., Elliott, M. A., Ruparel, K., Verma, R., Tunc, B., Gur, R. C., Gur, R. E., Bassett, D. S., & Satterthwaite, T. D. (2018). The impact of in-scanner head motion on structural connectivity derived from diffusion MRI. *NeuroImage*, *173*, 275–286.

Bedard, A.-C., Ickowicz, A., Logan, G. D., Hogg-Johnson, S., Schachar, R., & Tannock, R. (2003). Selective inhibition in children with attention-deficit hyperactivity disorder off and on stimulant medication. *Journal of Abnormal Child Psychology*, *31*, 315–327.

Bessette, K. L., & Stevens, M. C. (2019). Neurocognitive pathways in attention-deficit/hyperactivity disorder and white matter microstructure. *Biological Psychiatry: Cognitive Neuroscience and Neuroimaging*, *4*, 233–242.

Bhaijiwala, M., Chevrier, A., & Schachar, R. (2014). Withholding and canceling a response in ADHD adolescents. *Brain and Behavior: A Cognitive Neuroscience Perspective*, *4*, 602–614.

Bloemsma, J. M., Boer, F., Arnold, R., Banaschewski, T., Faraone, S. V., Buitelaar, J. K., Sergeant, J. A., Rommelse, N., & Oosterlaan, J. (2013). Comorbid anxiety and neurocognitive dysfunctions in children with ADHD. *European Child & Adolescent Psychiatry*, *22*, 225–234.

Boen, R., Ferschmann, L., Vijayakumar, N., Overbye, K., Fjell, A. M., Espeseth, T., & Tamnes, C. K. (2021). Development of attention networks from childhood to young adulthood: A study of performance, intraindividual variability and cortical thickness. *Cortex*, *138*, 138–151.

Brackenridge, R., McKenzie, K., Murray, G. C., & Quigley, A. (2011). An examination of the effects of stimulant medication on response inhibition: A comparison between children with and without attention deficit hyperactivity disorder. *Research in Developmental Disabilities*, *32*, 2797–2804.

Cai, W., Chen, T., Szegletes, L., Supekar, K., & Menon, V. (2018). Aberrant time-varying cross-network interactions in children with attention-deficit/hyperactivity disorder and the relation to attention deficits. *Biological Psychiatry: Cognitive Neuroscience and Neuroimaging*, *3*, 263–273.

Chen, L., Hu, X., Ouyang, L., He, N., Liao, Y., Liu, Q., Zhou, M., Wu, M., Huang, X., & Gong, Q. (2016). A systematic review and meta-analysis of tract-based spatial statistics studies regarding attention-deficit/hyperactivity disorder. *Neuroscience and Biobehavioral Reviews*, *68*, 838–847.

Chen, W., de Hemptinne, C., Miller, A. M., Leibbrand, M., Little, S. J., Lim, D. A., Larson, P. S., & Starr, P. A. (2020). Prefrontal-subthalamic Hyperdirect pathway modulates movement inhibition in humans. *Neuron*, *106*, 579–588.e3.

Choo, Y., Matzke, D., Bowren, M. D., Jr., Tranel, D., & Wessel, J. R. (2022). Right inferior frontal gyrus damage is associated with impaired initiation of inhibitory control, but not its implementation. *eLife*, *11*, e79667.

Claesdotter, E., Cervin, M., Kerlund, S., Rstam, M., & Lindvall, M. (2018). The effects of ADHD on cognitive performance. *Nordic Journal of Psychiatry*, *72*, 158–163.

Coghill, D. (2010). The impact of medications on quality of life in attention-deficit hyperactivity disorder: A systematic review. *CNS Drugs*, *24*, 843–866. https://doi.org/10.2165/11537450-000000000-00000

Curley, L. B., Newman, E., Thompson, W. K., Brown, T. T., Hagler, D. J., Jr., Akshoomoff, N., Reuter, C., Dale, A. M., & Jernigan, T. L. (2018). Cortical morphology of the pars opercularis and its relationship to motor-inhibitory performance in a longitudinal, developing cohort. *Brain Structure & Function*, *223*, 211–220.

Damatac, C. G., Chauvin, R. J. M., Zwiers, M. P., van Rooij, D., Akkermans, S. E. A., Naaijen, J., Hoekstra, P. J., Hartman, C. A., Oosterlaan, J., Franke, B., Buitelaar, J. K., Beckmann, C. F., & Sprooten, E. (2020). White matter microstructure in attention-deficit/hyperactivity disorder: A systematic Tractography study in 654 individuals. *Biological Psychiatry: Cognitive Neuroscience and Neuroimaging*, *7*, 979–988.

Dawson, M. R. W. (1988). Fitting the ex-Gaussian equation to reaction time distributions. *Behavior Research Methods, Instruments, & Computers*, *20*, 54–57.

de Zeeuw, P., Aarnoudse-Moens, C., Bijlhout, J., Knig, C., Uiterweer, A. P., Papanikolau, A., Hoogenraad, C., Im, t. L., de Been, D., Sergeant, J. A., & Oosterlaan, J. (2008). Inhibitory performance, response speed, intraindividual variability, and response accuracy in ADHD. *Journal of the American Academy of Child and Adolescent Psychiatry*, *47*, 808–816.

Dhollander, T., Clemente, A., Singh, M., Boonstra, F., Civier, O., Duque, J. D., Egorova, N., Enticott, P., Fuelscher, I., Gajamange, S., Genc, S., Gottlieb, E., Hyde, C., Imms, P., Kelly, C., Kirkovski, M., Kolbe, S., Liang, X., Malhotra, A., … Caeyenberghs, K. (2021). Fixel-based analysis of diffusion MRI: Methods, applications, challenges and opportunities. *NeuroImage*, *241*, 118417.

Dhollander, T., Raffelt, D., & Connelly, A. (2016). Unsupervised 3-tissue response function estimation from single-shell or multi-shell diffusion MR data without a co-registered T1 image. ISMRM Workshop on Breaking the Barriers of Diffusion MRI, Vol. 5.

Diesburg, D. A., & Wessel, J. R. (2021). The pause-then-cancel model of human action-stopping: Theoretical considerations and empirical evidence. *Neuroscience & Biobehavioral Reviews*, *129*, 17–34.

El-Sayed, E., Larsson, J.-O., Persson, H. E., Santosh, P. J., & Rydelius, P.-A. (2003). "Maturational lag" hypothesis of attention deficit hyperactivity disorder: An update. *Acta Paediatrica*, *92*, 776–784.

Faraone, S. V., Asherson, P., Banaschewski, T., Biederman, J., Buitelaar, J. K., Ramos-Quiroga, J. A., Rohde, L. A., Sonuga-Barke, E. J. S., Tannock, R., & Franke, B. (2015). Attention-deficit/hyperactivity disorder. *Nature Reviews. Disease Primers*, *1*, 1–23.

Fischl, B. (2012). FreeSurfer. *NeuroImage*, *62*, 774–781.

Fjell, A. M., Westlye, L. T., Amlien, I. K., & Walhovd, K. B. (2011). Reduced white matter integrity is related to cognitive instability. *The Journal of Neuroscience*, *31*, 18060–18072.

Fuelscher, I., Hyde, C., Anderson, V., & Silk, T. J. (2021). White matter tract signatures of fiber density and morphology in ADHD. *Cortex*, *138*, 329–340.

Gelman, A., & Rubin, D. B. (1992). Inference from iterative simulation using multiple sequences. *Statistical Science*, *7*, 457–472.

Genc, S., Malpas, C. B., Gulenc, A., Sciberras, E., Efron, D., Silk, T. J., & Seal, M. L. (2020). Longitudinal patterns of white matter fibre density and morphology in children are associated with age and pubertal stage. *Developmental Cognitive Neuroscience*, *45*, 100853.

Genc, S., Smith, R. E., Malpas, C. B., Anderson, V., Nicholson, J. M., Efron, D., Sciberras, E., Seal, M. L., & Silk, T. J. (2018). Development of white matter fibre density and morphology over childhood: A longitudinal fixel-based analysis. *NeuroImage*, *183*, 666–676.

Goddings, A.-L., Roalf, D., Lebel, C., & Tamnes, C. K. (2021). Development of white matter microstructure and executive functions during childhood and adolescence: A review of diffusion MRI studies. *Developmental Cognitive Neuroscience*, *51*, 101008.

Goscinski, W. J., McIntosh, P., Felzmann, U., Maksimenko, A., Hall, C. J., Gureyev, T., Thompson, D., Janke, A., Galloway, G., Killeen, N. E. B., Raniga, P., Kaluza, O., Ng, A., Poudel, G., Barnes, D. G., Nguyen, T., Bonnington, P., & Egan, G. F. (2014). The multi-modal Australian ScienceS imaging and visualization environment (MASSIVE) high performance computing infrastructure: Applications in neuroscience and neuroinformatics research. *Frontiers in Neuroinformatics*, *8*, 30.

Halliday, D. W., Kim, Y., MacDonald, S. W., Garcia-Barrera, M. A., Hundza, S. R., & Macoun, S. J. (2021). Intraindividual variability in executive and motor control tasks in children with attention deficit hyperactivity disorder. *Journal of Clinical and Experimental Neuropsychology*, *43*(6), 568–578.

Hampshire, A. (2015). Putting the brakes on inhibitory models of frontal lobe function. *NeuroImage*, *113*, 340–355.

Hampshire, A., Chamberlain, S. R., Monti, M. M., Duncan, J., & Owen, A. M. (2010). The role of the right inferior frontal gyrus: Inhibition and attentional control. *NeuroImage*, *50*, 1313–1319.

Hannah, R., & Aron, A. R. (2021). Towards real-world generalizability of a circuit for action-stopping. *Nature Reviews Neuroscience*, *22*, 538–552.

Hannah, R., Muralidharan, V., & Aron, A. R. (2023). Failing to attend versus failing to stop: Single-trial decomposition of action-stopping in the stop signal task. *Behavior Research Methods*, *55*(8), 4099–4117.

Hastie, T. J., & Tibshirani, R. J. (1990). *Generalized additive models* (Vol. 43). CRC Press.

Heathcote, A., Lin, Y.-S., Reynolds, A., Strickland, L., Gretton, M., & Matzke, D. (2019). Dynamic models of choice. *Behavior Research Methods*, *51*, 961–985.

Hyde, C., Sciberras, E., Efron, D., Fuelscher, I., & Silk, T. (2021). Reduced fine motor competence in children with ADHD is associated with atypical microstructural organization within the superior longitudinal fasciculus. *Brain Imaging and Behavior*, *15*, 727–737.

Jahfari, S., Waldorp, L., van den Wildenberg, W. P. M., Scholte, H. S., Ridderinkhof, K. R., & Forstmann, B. U. (2011). Effective connectivity reveals important roles for both the hyperdirect (fronto-subthalamic) and the indirect (fronto-striatal-pallidal) fronto-basal ganglia pathways during response inhibition. *The Journal of Neuroscience*, *31*, 6891–6899.

Jana, S., & Aron, A. R. (2022). Mind Wandering Impedes Response Inhibition by Affecting the Triggering of the Inhibitory Process. *Psychological Science*, *33*, 1068–1085. https://doi.org/10.1177/09567976211055371

Jana, S., Hannah, R., Muralidharan, V., & Aron, A. R. (2020). Temporal cascade of frontal, motor and muscle processes underlying human action-stopping. *eLife*, *9*, e50371.

Karalunas, S. L., & Huang-Pollock, C. L. (2013). Integrating impairments in reaction time and executive function using a diffusion model framework. *Journal of Abnormal Child Psychology*, *41*, 837–850.

Kellner, E., Dhital, B., Kiselev, V. G., & Reisert, M. (2016). Gibbs-ringing artifact removal based on local subvoxel-shifts. *Magnetic Resonance in Medicine*, *76*, 1574–1581.

Keuken, M. C., & Forstmann, B. U. (2015). A probabilistic atlas of the basal ganglia using 7 T MRI. *Data in Brief*, *4*, 577–582.

Kijonka, M., Borys, D., Psiuk-Maksymowicz, K., Gorczewski, K., Wojcieszek, P., Kossowski, B., Marchewka, A., Swierniak, A., Sokol, M., & Bobek-Billewicz, B. (2020). Whole brain and cranial size adjustments in volumetric brain analyses of sex- and age-related trends. *Frontiers in Neuroscience*, *14*, 278.

King, A. V., Linke, J., Gass, A., Hennerici, M. G., Tost, H., Poupon, C., & Wessa, M. (2012). Microstructure of a three-way anatomical network predicts individual differences in response inhibition: A tractography study. *NeuroImage*, *59*, 1949–1959.

Klein, C., Wendling, K., Huettner, P., Ruder, H., & Peper, M. (2006). Intra-subject variability in attention-deficit hyperactivity disorder. *Biological Psychiatry*, *60*, 1088–1097.

Kofler, M. J., Harmon, S. L., Aduen, P. A., Day, T. N., Austin, K., Spiegel, J., Irwin, L., & Sarver, D. E. (2018). Neurocognitive and behavioral predictors of social problems in ADHD: A Bayesian framework. *Neuropsychology*, *32*, 344–355.

Kofler, M. J., Irwin, L. N., Soto, E. F., Groves, N. B., Harmon, S. L., & Sarver, D. E. (2019). Executive functioning heterogeneity in pediatric ADHD. *Journal of Abnormal Child Psychology*, *47*, 273–286.

Kofler, M. J., Rapport, M. D., Sarver, D. E., Raiker, J. S., Orban, S. A., Friedman, L. M., & Kolomeyer, E. G. (2013). Reaction time variability in ADHD: A meta-analytic review of 319 studies. *Clinical Psychology Review*, *33*, 795–811.

Lambek, R., Tannock, R., Dalsgaard, S., Trillingsgaard, A., Damm, D., & Thomsen, P. H. (2011). Executive dysfunction in school-age children with ADHD. *Journal of Attention Disorders*, *15*, 646–655.

Last, B. S., Lawson, G. M., Breiner, K., Steinberg, L., & Farah, M. J. (2018). Childhood socioeconomic status and executive function in childhood and beyond. *PLoS One*, *13*, e0202964.

Lawson, G. M., Hook, C. J., & Farah, M. J. (2018). A meta-analysis of the relationship between socioeconomic status and executive function performance among children. *Developmental Science*, *21*, e12529.

Li, Q., Sun, J., Guo, L., Zang, Y.-F., Feng, Z., Huang, X., Yang, H., Lv, Y., Huang, M., & Gong, Q. (2010). Increased fractional anisotropy in white matter of the right frontal region in children with attention-

deficit/hyperactivity disorder: A diffusion tensor imaging study. *Neuro Endocrinology Letters*, *31*, 747–753.

Lijffijt, M., Kenemans, J. L., Verbaten, M. N., & van Engeland, H. (2005). A meta-analytic review of stopping performance in attention-deficit/hyperactivity disorder: Deficient inhibitory motor control? *Journal of Abnormal Psychology*, *114*, 216–222.

Lipszyc, J., & Schachar, R. (2010). Inhibitory control and psychopathology: A meta-analysis of studies using the stop signal task. *Journal of the International Neuropsychological Society*, *16*, 1064–1076.

Logan, G. D. (1994). On the ability to inhibit thought and action: A users' guide to the stop signal paradigm. In *Inhibitory processes in attention, memory, and language* (pp. 189–239). Academic Press.

Logan, G. D., & Cowan, W. B. (1984). On the ability to inhibit thought and action: A theory of an act of control. *Psychological Review*, *91*, 295–327.

Luna, F. G., Lupiáñez, J., & Martín-Arévalo, E. (2021). Microstructural white matter connectivity underlying the attentional networks system. *Behavioural Brain Research*, *401*, 113079.

Madsen, K. S. (2010). Response inhibition is associated with white matter microstructure in children. *Neuropsychologia*, *48*, 854–862. https://doi.org/10.1016/j.neuropsychologia.2009.11.001

Madsen, K. S., Johansen, L. B., Thompson, W. K., Siebner, H. R., Jernigan, T. L., & Baaré, W. F. C. (2020). Maturational trajectories of white matter microstructure underlying the right presupplementary motor area reflect individual improvements in motor response cancellation in children and adolescents. *NeuroImage*, *220*, 117105.

Mansouri, F. A., Fehring, D. J., Gaillard, A., Jaberzadeh, S., & Parkington, H. (2016). Sex dependency of inhibitory control functions. *Biology of Sex Differences*, *7*, 11.

Marek, S., Tervo-Clemmens, B., Calabro, F. J., Montez, D. F., Kay, B. P., Hatoum, A. S., Donohue, M. R., Foran, W., Miller, R. L., Hendrickson, T. J., Malone, S. M., Kandala, S., Feczko, E., Miranda-Dominguez, O., Graham, A. M., Earl, E. A., Perrone, A. J., Cordova, M., Doyle, O., … Dosenbach, N. U. F. (2022). Reproducible brain-wide association studies require thousands of individuals. *Nature*, *603*, 654–660.

Matzke, D., Curley, S., Gong, C. Q., & Heathcote, A. (2019). Inhibiting responses to difficult choices. *Journal of Experimental Psychology. General*, *148*, 124–142.

Matzke, D., Dolan, C. V., Logan, G. D., Brown, S. D., & Wagenmakers, E.-J. (2013). Bayesian parametric estimation of stop-signal reaction time distributions. *Journal of Experimental Psychology. General*, *142*, 1047–1073.

Matzke, D., Hughes, M., Badcock, J. C., Michie, P., & Heathcote, A. (2017). Failures of cognitive control or attention? The case of stop-signal deficits in schizophrenia. *Attention, Perception, & Psychophysics*, *79*, 1078–1086.

Matzke, D., Love, J., & Heathcote, A. (2017). A Bayesian approach for estimating the probability of trigger failures in the stop-signal paradigm. *Behavior Research Methods*, *49*, 267–281. https://doi.org/10.3758/s13428-015-0695-8

Matzke, D., Verbruggen, F., & Logan, G. D. (2018). The stop-signal paradigm. In *Stevens' handbook of experimental psychology and cognitive neuroscience* (pp. 1–45). American Cancer Society. https://doi.org/10.1002/9781119170174.epcn510

Mayes, W., Gentle, J., Parisi, I., Dixon, L., van Velzen, J., & Violante, I. (2021). Top-down inhibitory motor control is preserved in adults with developmental coordination disorder. *Developmental Neuropsychology*, *46*, 409–424.

Michelini, G., Kitsune, G. L., Cheung, C. H. M., Brandeis, D., Banaschewski, T., Asherson, P., McLoughlin, G., & Kuntsi, J. (2016). Attention-deficit/hyperactivity disorder remission is linked to better neurophysiological error detection and attention-vigilance processes. *Biological Psychiatry*, *80*, 923–932.

Mills, K. L., & Tamnes, C. K. (2014). Methods and considerations for longitudinal structural brain imaging analysis across development. *Developmental Cognitive Neuroscience*, *9*, 172–190.

Oosterlaan, J., Logan, G. D., & Sergeant, J. A. (1998). Response inhibition in AD/HD, CD, comorbid AD/HD+CD, anxious, and control children: A meta-analysis of studies with the stop task. *Journal of Child Psychology and Psychiatry*, *39*, 411–425.

Peterson, D. J., Ryan, M., Rimrodt, S. L., Cutting, L. E., Denckla, M. B., Kaufmann, W. E., & Mahone, E. M. (2011). Increased regional fractional anisotropy in highly screened attention-deficit hyperactivity disorder (ADHD). *Journal of Child Neurology*, *26*, 1296–1302.

Power, J. D., Barnes, K. A., Snyder, A. Z., Schlaggar, B. L., & Petersen, S. E. (2012). Spurious but systematic correlations in functional connectivity MRI networks arise from subject motion. *NeuroImage*, *59*, 2142–2154.

Rae, C. L., Hughes, L. E., Anderson, M. C., & Rowe, J. B. (2015). The prefrontal cortex achieves inhibitory control by facilitating subcortical motor pathway connectivity. *The Journal of Neuroscience*, *35*, 786–794. https://doi.org/10.1523/JNEUROSCI.3093-13.2015

Raffelt, D. A., Tournier, J. D., Smith, R. E., Vaughan, D. N., Jackson, G., Ridgway, G. R., & Connelly, A. (2017). Investigating white matter fibre density and morphology using fixel-based analysis. *NeuroImage*, *144*, 58–73.

Ramos, A. A., Hamdan, A. C., & Machado, L. (2020). A meta-analysis on verbal working memory in children and adolescents with ADHD. *The Clinical Neuropsychologist*, *34*(5), 873–898.

Ranta, M. E., Chen, M., Crocetti, D., Prince, J. L., Subramaniam, K., Fischl, B., Kaufmann, W. E., & Mostofsky, S. H. (2014). Automated MRI parcellation of the frontal lobe. *Human Brain Mapping*, *35*, 2009–2026.

Ribeiro, F., Cavaglia, R., & Rato, J. R. (2021). Sex differences in response inhibition in young children. *Cognitive Development*, *58*, 101047.

Salum, G. A., Sato, J. R., Manfro, A. G., Pan, P. M., Gadelha, A., do Rosário, M. C., Polanczyk, G. V., Castellanos, F. X., Sonuga-Barke, E., & Rohde, L. A. (2019). Reaction time variability and attention-deficit/hyperactivity disorder: Is increased reaction time variability specific to attention-deficit/hyperactivity disorder? Testing predictions from the default-mode interference hypothesis. *Attention Deficit and Hyperactivity Disorders*, *11*, 47–58.

Sciberras, E., Efron, D., Schilpzand, E. J., Anderson, V., Jongeling, B., Hazell, P., Ukoumunne, O. C., & Nicholson, J. M. (2013). The Children's attention project: A community-based longitudinal study of children with ADHD and non-ADHD controls. *BMC Psychiatry*, *13*, 1–11.

Shaffer, D., Fisher, P., Lucas, C. P., Dulcan, M. K., & Schwab-Stone, M. E. (2000). NIMH diagnostic interview schedule for children version IV (NIMH DISC-IV): Description, differences from previous versions, and reliability of some common diagnoses. *Journal of the American Academy of Child and Adolescent Psychiatry*, *39*, 28–38.

Shaw, P. (2007). Attention-deficit/hyperactivity disorder is characterized by a delay in cortical maturation. *Proceedings of the National Academy of Sciences of the United States of America*, *104*, 19649–19654. https://doi.org/10.1073/pnas.0707741104

Shaw, P. (2013). Trajectories of cerebral cortical development in childhood and adolescence and adult attention-deficit/hyperactivity disorder. *Biological Psychiatry*, *74*, 599–606. https://doi.org/10.1016/j.biopsych.2013.04.007

Shiels, K., Tamm, L., & Epstein, J. N. (2012). Deficient post-error slowing in children with ADHD is limited to the inattentive subtype. *Journal of the International Neuropsychological Society*, *18*, 612–617.

Silk, T. J., Genc, S., Anderson, V., Efron, D., Hazell, P., Nicholson, J. M., Kean, M., Malpas, C. B., & Sciberras, E. (2016). Developmental brain trajectories in children with ADHD and controls: A longitudinal neuroimaging study. *BMC Psychiatry*, *16*, 1–9.

Singh, M., Fuelscher, I., He, J., Anderson, V., Silk, T. J., & Hyde, C. (2021). Inter-individual performance differences in the stop-signal task are

associated with fibre-specific microstructure of the fronto-basal-ganglia circuit in healthy children. *Cortex*, *142*, 283–295.

Singh, M., Skippen, P., He, J., Thomson, P., Fuelscher, I., Caeyenberghs, K., Anderson, V., Nicholson, J. M., Hyde, C., & Silk, T. J. (2022). Longitudinal developmental trajectories of inhibition and white-matter maturation of the fronto-basal-ganglia circuits. *Developmental Cognitive Neuroscience*, *58*, 101171.

Skippen, P. (2019). Reliability of triggering inhibitory process is a better predictor of impulsivity than SSRT. *Acta Psychologica*, *192*, 104–117. https://doi.org/10.1016/j.actpsy.2018.10.016

Slaats-Willemse, D., Swaab-Barneveld, H., de Sonneville, L., van der Meulen, E., & Buitelaar, J. (2003). Deficient response inhibition as a cognitive endophenotype of ADHD. *Journal of the American Academy of Child and Adolescent Psychiatry*, *42*, 1242–1248.

Sripada, C. S., Kessler, D., & Angstadt, M. (2014). Lag in maturation of the brain's intrinsic functional architecture in attention-deficit/hyperactivity disorder. *Proceedings of the National Academy of Sciences of the United States of America*, *111*, 14259–14264.

Sudre, G., Norman, L., Bouyssi-Kobar, M., Price, J., Shastri, G. G., & Shaw, P. (2023). A Mega-analytic Study of White Matter Microstructural Differences Across 5 Cohorts of Youths With Attention-Deficit/Hyperactivity Disorder. *Biological Psychiatry*, *94*(1), 18–28. https://doi.org/10.1016/j.biopsych.2022.09.021

Tamnes, C. K., Fjell, A. M., Westlye, L. T., Østby, Y., & Walhovd, K. B. (2012). Becoming consistent: Developmental reductions in Intraindividual variability in reaction time are related to white matter integrity. *The Journal of Neuroscience*, *32*, 972–982.

Thomson, P., Johnson, K. A., Malpas, C. B., Efron, D., Sciberras, E., & Silk, T. J. (2021). Head motion during MRI predicted by out-of-scanner sustained attention performance in attention-deficit/hyperactivity disorder. *Journal of Attention Disorders*, *25*, 1429–1440.

Thomson, P., Malpas, C. B., Vijayakumar, N., Johnson, K. A., Anderson, V., Efron, D., Hazell, P., & Silk, T. J. (2022). Longitudinal maturation of resting state networks: Relevance to sustained attention and attention deficit/hyperactivity disorder. *Cognitive, Affective, & Behavioral Neuroscience*, *22*, 1432–1446. https://doi.org/10.3758/s13415-022-01017-9

Thomson, P., Vijayakumar, N., Fuelscher, I., Malpas, C. B., Hazell, P., & Silk, T. J. (2022). White matter and sustained attention in children with attention/deficit-hyperactivity disorder: A longitudinal fixel-based analysis. *Cortex*, *157*, 129–141.

Tournier, J. D., Smith, R., Raffelt, D., Tabbara, R., Dhollander, T., Pietsch, M., Christiaens, D., Jeurissen, B., Yeh, C.-H., & Connelly, A. (2019). MRtrix3: A fast, flexible and open software framework for medical image processing and visualisation. *NeuroImage*, *202*, 116137.

Tremblay, L. K., Hammill, C., Ameis, S. H., Bhaijiwala, M., Mabbott, D. J., Anagnostou, E., Lerch, J. P., & Schachar, R. J. (2020). Tracking inhibitory control in youth with ADHD: A multi-modal neuroimaging approach. *Frontiers in Psychiatry*, *11*, 00831.

Turner, B. M., Sederberg, P. B., Brown, S. D., & Steyvers, M. (2013). A method for efficiently sampling from distributions with correlated dimensions. *Psychological Methods*, *18*, 368–384.

Uebel, H., Albrecht, B., Asherson, P., Börger, N. A., Butler, L., Chen, W., Christiansen, H., Heise, A., Kuntsi, J., Schäfer, U., Andreou, P., Manor, I., Marco, R., Miranda, A., Mulligan, A., Oades, R. D., Meere, J. V. D., Faraone, S. V., Rothenberger, A., & Banaschewski, T. (2010). Performance variability, impulsivity errors and the impact of incentives as gender-independent endophenotypes for ADHD. *Journal of Child Psychology and Psychiatry*, *51*, 210–218.

van de Schoot, R., Kaplan, D., Denissen, J., Asendorpf, J. B., Neyer, F. J., & van Aken, M. A. G. (2014). A Gentle introduction to Bayesian analysis: Applications to developmental research. *Child Development*, *85*, 842–860.

van Rij, J., Wieling, M., Baayen, R. H., & van Rijn, D. (2015). Itsadug: Interpreting time series and autocorrelated data using GAMMs. R package version 2.4.1.

Veraart, J., Novikov, D. S., Christiaens, D., Ades-aron, B., Sijbers, J., & Fieremans, E. (2016). Denoising of diffusion MRI using random matrix theory. *NeuroImage*, *142*, 394–406.

Verbruggen, F. (2019). A consensus guide to capturing the ability to inhibit actions and impulsive behaviors in the stop-signal task. *eLife*, *8*, e46323. https://doi.org/10.7554/eLife.46323

Verbruggen, F., & Logan, G. D. (2008). Response inhibition in the stop-signal paradigm. *Trends in Cognitive Sciences*, *12*, 418–424.

Verbruggen, F., & Logan, G. D. (2009). Models of response inhibition in the stop-signal and stop-change paradigms. *Neuroscience and Biobehavioral Reviews*, *33*, 647–661.

Verbruggen, F., Logan, G. D., & Stevens, M. A. (2008). STOP-IT: Windows executable software for the stop-signal paradigm. *Behavior Research Methods*, *40*, 479–483.

Vijayakumar, N., Youssef, G. J., Allen, N. B., Anderson, V., Efron, D., Hazell, P., Mundy, L., Nicholson, J. M., Patton, G., Seal, M. L., Simmons, J. G., Whittle, S., & Silk, T. (2021). A longitudinal analysis of puberty-related cortical development. *NeuroImage*, *228*, 117684.

Weigard, A., Heathcote, A., Matzke, D., & Huang-Pollock, C. (2019). Cognitive modeling suggests that attentional failures drive longer stop-signal reaction time estimates in attention deficit/hyperactivity disorder. *Clinical Psychological Science*, *7*, 856–872.

Willcutt, E. G. (2012). The prevalence of DSM-IV attention-deficit/hyperactivity disorder: A meta-analytic review. *Neurotherapeutics*, *9*, 490–499.

Williams, B. R., Ponesse, J. S., Schachar, R. J., Logan, G. D., & Tannock, R. (1999). Development of inhibitory control across the life span. *Developmental Psychology*, *35*, 205–213.

Wood, S. N. (2011). Fast stable restricted maximum likelihood and marginal likelihood estimation of semiparametric generalized linear models. *Journal of the Royal Statistical Society, Series B (Statistical Methodology)*, *73*, 3–36.

Wood, S. N. (2017). *Generalized additive models: An introduction with R*. CRC Press.

Zhang, R., Geng, X., & Lee, T. M. C. (2017). Large-scale functional neural network correlates of response inhibition: An fMRI meta-analysis. *Brain Structure & Function*, *222*, 3973–3990.

Zhao, C., Tapera, T. M., Bagautdinova, J., Bourque, J., Covitz, S., Gur, R. E., Gur, R. C., Larsen, B., Mehta, K., Meisler, S. L., Murtha, K., Muschelli, J., Roalf, D. R., Sydnor, V. J., Valcarcel, A. M., Shinohara, R. T., Cieslak, M., & Satterthwaite, T. D. (2023). ModelArray: An R package for statistical analysis of fixel-wise data. *NeuroImage*, *271*, 120037.

SUPPORTING INFORMATION

Additional supporting information can be found online in the Supporting Information section at the end of this article.

How to cite this article: Singh, M., Skippen, P., He, J., Thomson, P., Fuelscher, I., Caeyenberghs, K., Anderson, V., Hyde, C., & Silk, T. J. (2024). Developmental patterns of inhibition and fronto-basal-ganglia white matter organisation in healthy children and children with attention-deficit/hyperactivity disorder. *Human Brain Mapping*, *45*(15), e70010. https://doi.org/10.1002/hbm.70010